# Supporting Information for:

## Oligothienyl catenated germanes and silanes: synthesis, structure, properties

**Kirill V. Zaitsev,*[a] Kevin Lam, *[b] Oleg Kh. Poleshchuk,[c,d] Lyudmila G. Kuz'mina,[e] Andrei V. Churakov[e]**

[a] *Department of Chemistry, Moscow State University, Leninskye Gory 1, Moscow 119991, Russia. Fax: +7(495)932 8846; Tel: +7(495)939 3887*
[b] *Department of Pharmaceutical, Chemical and Environmental Sciences, Faculty of Engineering and Science, University of Greenwich, Central Avenue, Chatham Maritime, Chatham, Kent ME4 4TB, United Kingdom*
[c] *National Research Tomsk Polytechnic University, Lenin Av., 30, Tomsk, Russia*
[d] *Tomsk State Pedagogical University, Kievskaya Str., 60, Tomsk, Russia*
[e] *Russian Academy of Sciences, N.S. Kurnakov General and Inorganic Chemistry Institute, Leninskii pr., 31, Moscow, Russia*

*E-mail: k.lam@greenwich.ac.uk (KL); zaitsev@org.chem.msu.ru (KVZ)*

Table of Contents:

## *NMR spectra of oligothienyl catenated Group 14 derivatives*



## *UV/vis absorption and luminescence spectra*



## *DFT calculations*

## *Electrochemical data according to CV*

# *Synthetic procedures*

## Synthesis of initial germanium derivatives

**Dimethyldiphenylgermane, $Me_2GePh_2$.** The solution of $Ph_2GeCl_2$ (28.68 g, 96.30 mmol) in $Et_2O$ (50 ml) was added dropwise to the solution of the MeMgI in ether (80 ml) prepared by typical way from MeI (19.12 ml, 43.60 g, 307.00 mmol) and Mg (6.86 g, 282.20 mmol). After reflux for 2 h the reation mixture was poured into the saturated aq. solution of $NH_4Cl$, water phase was extracted with ether (3x50 ml), dried over $MgSO_4$. Then all volatile materials were removed under reduced pressure, and the residue was purified by distillation. Dimethyldiphenylgermane (20.78 g, 84 %) was isolated as colorless liquid. B.p. 125-126 $^oC$ (3 mm Hg),[1] b.p. 93-94 (3 mm Hg). NMR data corresponds to literature data.[2] $^1H$ NMR ($\delta$, ppm, $CDCl_3$): 7.58-7.54 (m, 4H), 7.43-7.40 (m, 6H) (aromatic protons), 0.72 (s, 6H, $GeMe_2$). $^{13}C$ NMR ($\delta$, ppm, $CDCl_3$): 140.20 (quaternary aromatic carbon), 133.62, 128.05 (aromatic *o*/*m*-CH carbons), 128.56 (aromatic *p*-CH carbon), -3.14 ($GeMe_2$).

**Bromodimethylphenylgermane, $Me_2GePhBr$.** The solution of dry bromine (2.00 ml, 6.22 g, 38.92 mmol) distilled over $P_4O_{10}$ in 1,2-dibromoethane (5 ml) was added dropwise to the solution of $Ph_2GeMe_2$ (10.00 g, 38.92 mmol) 1,2-dibromoethane (30 ml) at 85 $^oC$. The mixture obtained was refluxed for 2 h, then all volatile materials were removed under reduced pressure. The target compound (7.88 g, 78 %) was isolated by distillation. Colorless liquid. B.p. 63-65 $^oC$ (4 mm Hg). $^1H$ NMR ($\delta$, ppm, $CDCl_3$): 7.65-7.61 (m, 2H), 7.47-7.42 (m, 3H) (aromatic protons), 1.10 (s, 6H, $GeMe_2$). $^{13}C$ NMR ($\delta$, ppm, $CDCl_3$): 138.26 (quaternary aromatic carbon), 132.33, 128.42 (aromatic *o*/*m*-CH carbons), 130.02 (aromatic *p*-CH carbon), 4.00 ($GeMe_2$).

**Dimethylphenylgermane, $Me_2GePhH$.** $LiAlH_4$ (2.19 g, 57.76 mmol) was added dropwise to the solution of $Me_2GePhBr$ (10.00 g, 38.50 mmol) in ether (100 ml). After reflux during 2 h, saturated aq. solution of $NH_4Cl$ was added, water phase was ectracted with ether (3x30 ml), dried over $MgSO_4$, and then all volatile materials were removed under reduced pressure. The target compound (5.85 g, 84 %) was isolated by distillation. Colorless liquid, b.p. 80 $^oC$ (50 mm Hg),[3] b.p. 98-99 (64 mm Hg). $^1H$ NMR ($\delta$, ppm, $CDCl_3$): 7.52-7.47 (m, 2H), 7.36-7.31 (m, 3H) (aromatic protons), 4.47 (sept, $^3J_{H-H}$ = 3.5 Hz, 1H), 0.47 (s, 6H, $GeMe_2$). $^{13}C$ NMR ($\delta$, ppm, $CDCl_3$): 139.54 (quaternary aromatic carbon), 133.67, 128.04 (aromatic *o*/*m*-CH carbons), 128.48 (aromatic *p*-CH carbon), -4.32 ($GeMe_2$).

**Pentamethylphenyldigermane, $Me_3GeGeMe_2Ph$.** At 0$^oC$ to the solution of $Me_2GePhH$ (4.00 g, 22.12 mm`ol) in ether (30 ml) *n*-BuLi (8.85 ml, 2.5 M in *n*-hexane, 22.12 mmol) was added slowly, and then reaction mixture was stirred at room temperature for 3 h. The solution of $Me_3GeBr$ (2.84 ml, 4.37 g, 22.12 mmol) in ether (20 ml) was added to the solution of $Me_2GePhLi$ obtained as described earlier. After stirring overnight aq. saturated solution of $NH_4Cl$ was added, organic phase was extracted with ether (3x20 ml), dried over $MgSO_4$, and then all volatile materials were removed under reduced pressure. The target compound (5.53 g, 84%) was isolated by distillation on oil. Colorless oil, b.p. 82-84 $^oC$; b.p. 120 (8),[4] 110 (12).[5] UV/vis ($CH_2Cl_2$) $\lambda_{max}$ nm ($\varepsilon$, $M^{-1}$ $см^{-1}$): 230 ($3.4\times10^4$). $^1H$ NMR ($\delta$, ppm, $CDCl_3$): 7.45-7.40 (m, 2H), 7.35-7.30 (m, 3H) (aromatic protons), 0.47 (s, 6H, $GeMe_2$), 0.25 (s, 9H, $GeMe_3$). $^{13}C$ NMR ($\delta$, ppm, $CDCl_3$): 142.10 (quaternary aromatic carbon), 133.41, 128.88 (aromatic *o*/*m*-CH carbons), 127.79 (aromatic *p*-CH carbon), -2.23, -3.85 (2GeMe).

**Pentamethyldigermyl triflate, $Me_3GeGeMe_2OTf$.** At 0°C HOTf (0.883 ml, 9.98 mmol) was added to the solution of $Me_3GeGeMe_2Ph$ (2.91 g, 9.78 mmol) in $CH_2Cl_2$ (20 ml). Reaction mixture was stirred overnight overnight at room temperature, and then all volatile materials were removed under reduced pressure giving the target compound (3.39 g, 98%) as colorless oil. $^1$H NMR ($\delta$, ppm, $CDCl_3$): 0.88 (s, 6H, $GeMe_2$), 0.47 (s, 9H, $GeMe_3$). $^{13}$C NMR ($\delta$, ppm, $CDCl_3$): 118.76 ($^1J_{C\text{-}F}$ = 317.6 Hz, $CF_3$), 4.00, -2.36 (2GeMe). $^{19}$F NMR ($\delta$, ppm, $CDCl_3$): -77.63 (s).

**Chloropentamethyldigermane, $Me_3GeGeMe_2Cl$.** Finely ground $NH_4Cl$ (5.50 g, 102.80 mmol) dried over $P_4O_{10}$ was added to the solution of $Me_3GeGeMe_2OTf$ (5.50 g, 14.88 mmol) in $CH_2Cl_2$ (60 ml). The reaction mixture was stirred overnight, and then all volatile materials were removed under reduced pressure. The target compound (3.27 g, 86 %) was isolated by distillation, b.p. 72-73 (28 mm Hg). Colorless liquid. NMR data corresponds to literature data.[6] B.p. 64-65 (15),[7] 62-63 (18).[8] $^1$H NMR ($\delta$, ppm, $CDCl_3$): 0.75 (s, 6H, $GeMe_2$), 0.39 (s, 9H, $GeMe_3$). $^{13}$C NMR ($\delta$, ppm, $CDCl_3$): 4.53 ($GeMe_2$), -2.48 ($GeMe_3$).

## Synthesis of thienyl compounds

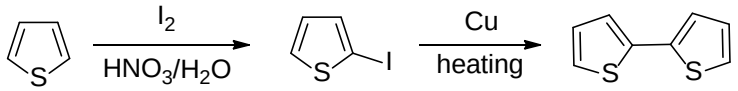


2,2'-$Th_2$

**2-Iodothiophene.**[9]

Freshly distilled thiopene (42.00 g, 39.00 ml, 500.00 mmol) and iodine (38.00 g, 150.00 mmol) were placed in a three-necked flask (250 ml) equipped with reflux condenser, dropping funnel. At vigorous stirring a mixture of $HNO_3$ concentrated (27.72 g, 440.00 mmol, 59%, d 1.352 g/ml) and water (21.00 ml) was added dropwise at internal temperature below 40 °C. The mixture obtained was refluxed for 0.5 h, then organic layer was separated and mixed with 10 % aq. NaOH. Organic phase was separated, dried over $MgSO_4$ and distilled. 2-Iodothiophene (6.93 g, 44 %) was isolated as yellowish oil, b. p. 71-71 °C (12 mm Hg).

$^1$H NMR ($\delta$, ppm, $CDCl_3$): 7.38 (dd, $^3J_{H\text{-}H}$ = 5.5 Hz, $^4J_{H\text{-}H}$ = 1.3 Hz, 1H), 7.28 (dd, $^3J_{H\text{-}H}$ = 3.5 Hz, $^4J_{H\text{-}H}$ = 1.3 Hz, 1H), 6.83 (dd, $^3J_{H\text{-}H}$ = 3.5 Hz, $^3J_{H\text{-}H}$ = 5.5 Hz, 1H) (thienyl protons). $^{13}$C NMR ($\delta$, ppm, $CDCl_3$): 136.82, 131.44, 128.81 (3 thienyl *C*H carbons), 73.10 (thienyl *C*I carbons).

**2,2'-Bithiophene (2,2'-$Th_2$).**[10]

The mixture of 2-iodothiophene (13.75 g, 65.00 mmol), copper bronze (4.45 g, 70.00 mmol) and DMF (20 ml) was refluxed for 12 h. Then water (50 ml) and $CH_2Cl_2$ (100 ml) was added, and mixture obtained was filtered. Organic phase was washed with water (5x50 ml), dried over $MgSO_4$, and then all volatile materials were removed under reduced pressure. The residue was distilled, and the fraction, b.p. 102-108 °C (4 mm Hg) was collected, and then recrystallized from *n*-hexane. 2,2'-$Th_2$ (7.78 g, 72 %) was isolated as yellowish crystals, m.p. 33-34 °C.

$^1$H NMR ($\delta$, ppm, $CDCl_3$): 7.21 (dd, $^4J_{H\text{-}H}$ = 1.2 Hz, $^3J_{H\text{-}H}$ = 5.1 Hz, 2H), 7.19 (dd, $^4J_{H\text{-}H}$ = 1.2 Hz, $^3J_{H\text{-}H}$ = 3.5 Hz, 2H), 7.02 (dd, $^3J_{H\text{-}H}$ = 3.5 Hz, $^3J_{H\text{-}H}$ = 5.1 Hz, 2H) (thienyl protons). $^{13}$C NMR ($\delta$, ppm, $CDCl_3$): 137.33 (quaternary thienyl carbon), 127.70, 124.28, 123.70 (thienyl CH carbons).

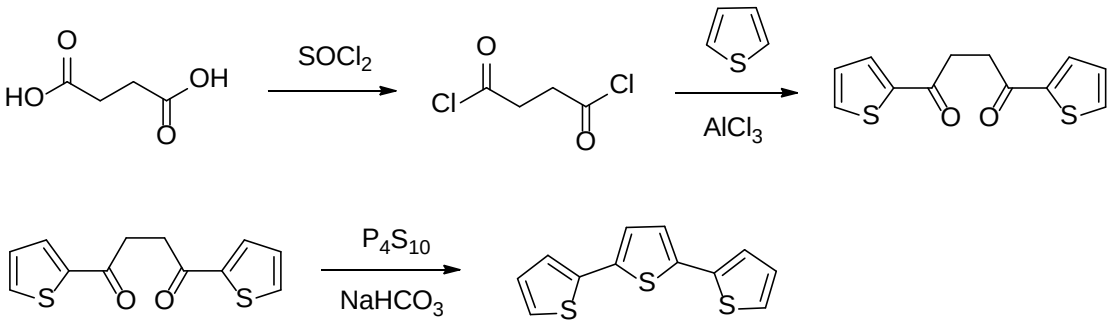


**1,4-Di-(2-thienyl)-1,4-butanedione**

a) **Synthesis of succinyl chloride.** Succinic acid (29.64 g, 251.00 mmol) was added portionwise to the $SOCl_2$ (60 ml, 97.86 g, 822.56 mmol). After reflux for 4 h, all volatile compounds were removed under reduced pressure. The residue obtained (38.62 g, >99%) was used further without purification.

b) **Synthesis of 1,4-Di-(2-thienyl)-1,4-butanedione.**[11] At 0°C the solution of thiophene (48.00 ml, 602.4 mmol) and succinyl chloride (38.62 g, 248.49 mmol) in $CH_2Cl_2$ (75 ml) obtained as described above was added dropwise to the suspension of $AlCl_3$ (80.32 g, 602.40 mmol) in $CH_2Cl_2$ (75 ml). Reaction mixture was stirred for 18 h, then poured into mixture of ice (400 g) and concentrated HCl (30 ml). Then organic phase was separated, washed with water (2x50 ml), aq. $NaHCO_3$ and dried over $MgSO_4$. After removing all volatile materials the residue was treated with EtOH (100 ml), filtered off and recrystallized with charcoal from toluene. Greenish powder (30.16 g, 48 %), m. p. 130-131 °C. $^1$H NMR ($\delta$, ppm, $CDCl_3$): 7.78 (dd, $^3J_{H-H}$ 3.9 Hz, $^4J_{H-H}$ 0.9 Hz 2H), 7.61 (dd, $^3J_{H-H}$ = 5.0 Hz, $^4J_{H-H}$ = 0.9 Hz, 2H), 7.10 (dd, $^3J_{H-H}$ = 5.0 Hz, $^3J_{H-H}$ = 3.9 Hz, 2H) (thienyl protons). $^{13}$C NMR ($\delta$, ppm, $CDCl_3$): 191.21 (C=O), 143.60 (quaternary thienyl carbon), 133.50, 131.98, 128.03 (thienyl CH carbons), 33.01 ($CH_2$).

**2,2',5',2''-Terthienyl (2,2':5',2''-Th$_3$)**[12]

$P_4S_{10}$ (11.11 g, 25.00 mmol) was added portionwise to the suspension of 1,4-di-(2-thienyl)-1,4-butanedione (5.00 g, 20.00 mmol) in ether (50 ml). Then $NaHCO_3$ (10.08 g, 120.00 mmol) was added portionwise so that $CO_2$ evolved slowly. After stirring for 3 h water (50 ml) was added, the mixture was filtered, and water phase was extracted with $CH_2Cl_2$ (3x40 ml), dried over $MgSO_4$. Then all volatile materials were removed under reduced pressure. The residue was purified by chromatogtaphy ($SiO_2$, petroleum ether, $R_f$ 0.3), and recrystallized from MeOH. Target compound (4.07 g, 82 %) was isolated as yellowish plates, m.p. 93-94 °C. $^1$H NMR ($\delta$, ppm, $CDCl_3$): 7.20 (dd, $^4J_{H-H}$ 1.2 Hz, $^3J_{H-H}$ 5.1 Hz, 2H), 7.16 (dd, $^3J_{H-H}$ = 3.7 Hz, $^4J_{H-H}$ = 1.2 Hz, 2H), 7.06 (s, 2H), 7.10 (dd, $^3J_{H-H}$ = 5.1 Hz, $^3J_{H-H}$ = 3.7 Hz, 2H) (thienyl protons). $^{13}$C NMR ($\delta$, ppm, $CDCl_3$): 137.20, 136.23 (2 quaternary thienyl carbons), 127.85, 124.47, 124.34, 123.74 (thienyl CH carbons).

**References**


1. M. Kumada, M. Ishikawa, S. Sakamoto, S. Maeda, *J. Organomet. Chem.* **1969,** *17* (2), 223.
2. K. L. Bobbitt, V. M. Maloney, P. P. Gaspar, *Organometallics* **1991,** *10* (8), 2772.
3. J. Escudie, C. Couret, J. Satge, J. D. Andriamizaka, *Organometallics* **1982,** *1* (10), 1261.
4. P. Riviére, J. Satgé, *Synth. React. Inorg. Met.-Org. Chem.* **1971,** *1* (1), 13.
5. A. Castel, P. Riviere, B. Saintroch, J. Satge, J. P. Malrieu, *J. Organomet. Chem.* **1983,** *247* (2), 149.
6. C. H. Yoder, J. E. Crouse, D. A. Wilson, *J. Organomet. Chem.* **1984,** *276* (1), 9.
7. K. Yamamoto, M. Kumada, *J. Organomet. Chem.* **1972,** *35* (2), 297.
8. E. J. Bulten, J. G. Noltes, *J. Organomet. Chem.* **1968,** *15* (2), P18.
9. H.Y. Lew, C.R. Noller, *Org. Synth.*, **1963**, *Coll. Vol. 5*, 545; **1950**, *30*, 53.
10. H. Wynberg, A. Logothetis, *J. Am. Chem. Soc.*, **1956**, *78*, 1958.
11. A. Merz, F. Ellinger, *Synthesis*, **1991**, 462.
12. H. Wynberg, J. Metselaar, *Synth. Commun.*, **1984**, *14*, 1.

# *Crystallographic Data*

## Description of the Experiment

Experimental intensities for **2a**, **2b**, **3a** and **3b** were measured on a Bruker SMART APEX II diffractometer (graphite monochromatized Mo-*K*α radiation, λ= 0.71073 Å) using $\omega$ scan mode. The structures were solved by direct methods and refined by full matrix least-squares on $F^2$ (*SHELXTL*) with anisotropic thermal parameters for all non-hydrogen atoms. Hydrogen atoms were placed in calculated positions and refined using a riding model. In **2a** $SiMe_3$ group is rotationally disordered over two positions with occupancy ratio 0.80(1)/0.20(1).

Crystal data, data collection, structure solution and refinement parameters are listed in Table S-1. Crystallographic data for the structures reported in this paper have been deposited with the Cambridge Crystallographic Data Centre as supplementary publications no. CCDC-1810961-1810964.

**Table S1.** Crystallographic Data for Compounds **2a**, **2b**, **3a** and **3b**.

| | **2a** | **2b** | **3a** | **3b** |
|---|---|---|---|---|
| empirical formula | $C_{18}H_{34}S_2Si_4$ | $C_{18}H_{34}Ge_4S_2$ | $C_{20}H_{22}S_4Si_2$ | $C_{20}H_{22}Ge_2S_4$ |
| $M_w$ | 426.93 | 604.93 | 446.80 | 535.80 |
| temperature (K) | 150(2) | 170(2) | 150(2) | 150(2) |
| size (mm) | 0.35 x 0.20 x 0.10 | 0.38 x 0.32 x 0.26 | 0.25 x 0.20 x 0.20 | 0.20 x 0.15 x 0.10 |
| cryst. system | triclinic | triclinic | monoclinic | monoclinic |
| space group | *P*-1 | *P*-1 | $P2_1/c$ | $P2_1/c$ |
| *a* (Å) | 6.6294(5) | 6.7760(10) | 7.6131(4) | 7.6171(3) |
| *b* (Å) | 6.7581(5) | 8.4190(13) | 8.7828(4) | 8.9311(4) |
| *c* (Å) | 14.6108(11) | 12.5300(19) | 16.7001(8) | 16.6999(7) |
| $\alpha$ (deg) | 85.8080(10) | 90.805(2) | 90 | 90 |
| $\beta$ (deg) | 81.3960(10) | 94.883(2) | 95.931(1) | 96.6462(6) |
| $\gamma$ (deg) | 79.9180(10) | 112.136(2) | 90 | 90 |
| V (Å$^3$) | 636.49(8) | 658.89(17) | 1110.66(9) | 1128.44(8) |
| Z | 1 | 1 | 2 | 2 |
| $\rho_{cald}$ (g*cm$^{-3}$) | 1.114 | 1.525 | 1.336 | 1.577 |
| abs coeff. (mm$^{-1}$) | 0.398 | 4.676 | 0.539 | 3.036 |
| *F*(000) | 230 | 302 | 468 | 540 |
| $\theta$ range (deg) | 3.07 – 27.00 | 2.62- 29.00 | 2.45 - 29.00 | 2.46 – 29.00 |
| no. of collected/unique rflns. | 6151 / 2763 | 7182 / 3464 | 12179 / 2951 | 12365 / 3001 |
| $R_{int}$ | 0.0107 | 0.0173 | 0.0155 | 0.0159 |
| data/restraints/params. | 2763/ 30 / 135 | 3464/ 0 / 114 | 2951 / 1 / 120 | 3001 / 1 / 120 |
| goodness of fit on $F^2$ | 1.064 | 1.099 | 1.075 | 1.064 |
| final *R* indices ($I > 2\sigma(I)$) | $R_1$ = 0.0257, $wR_2$ = 0.0704 | $R_1$ = 0.0302, $wR_2$ = 0.0782 | $R_1$ = 0.0284, $wR_2$ = 0.0838 | $R_1$ = 0.0187, $wR_2$ = 0.0536 |
| *R* indices (all data) | $R_1$ = 0.0278, $wR_2$ = 0.0724 | $R_1$ = 0.0408, $wR_2$ = 0.0814 | $R_1$ = 0.0307, $wR_2$ = 0.0860 | $R_1$ = 0.0200, $wR_2$ = 0.0544 |
| largest diff. peak/hole (e/Å$^3$) | 0.335 / -0.243 | 1.204 / -0.466 | 0.531 / -0.511 | 0.583 / -0.551 |

# ***Spectral NMR Data***

## *NMR spectra of initial germanium compounds*

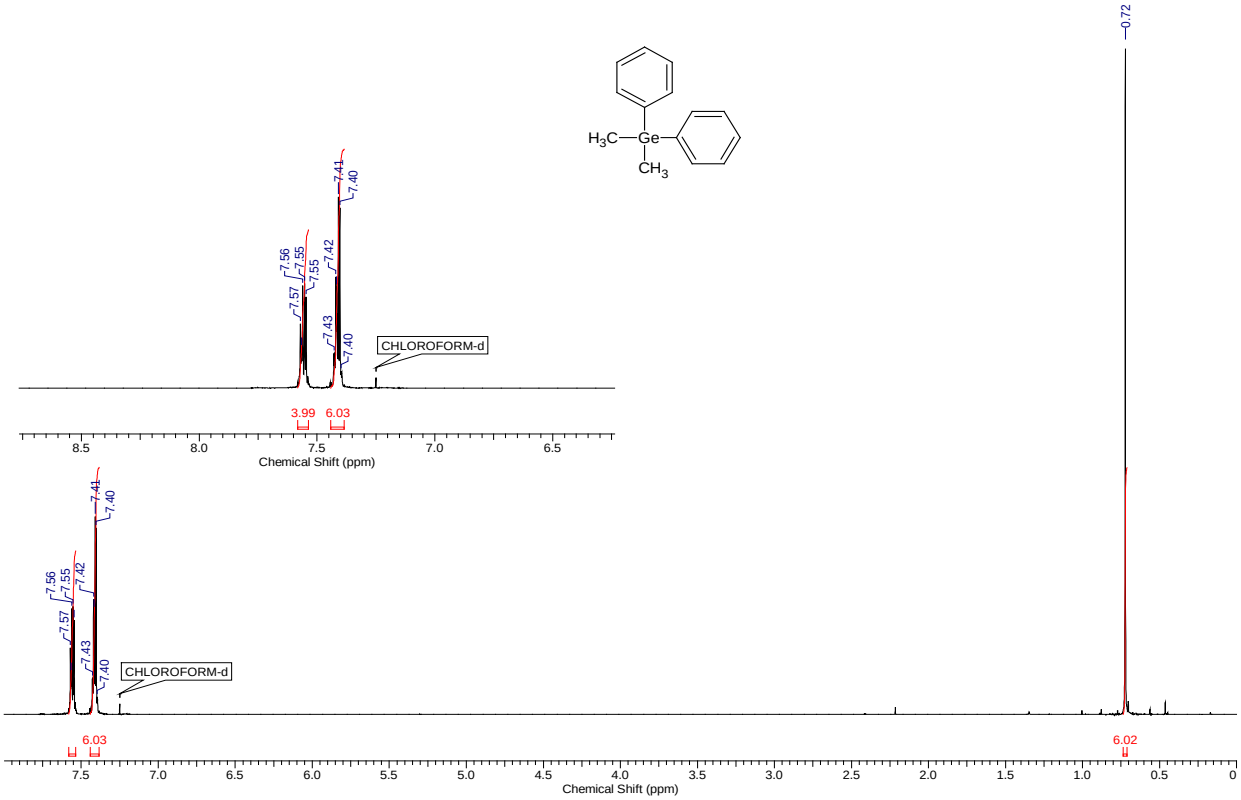


**Figure S1.** $^{1}$H NMR spectrum for $Me_2GePh_2$ ($CDCl_3$, RT).

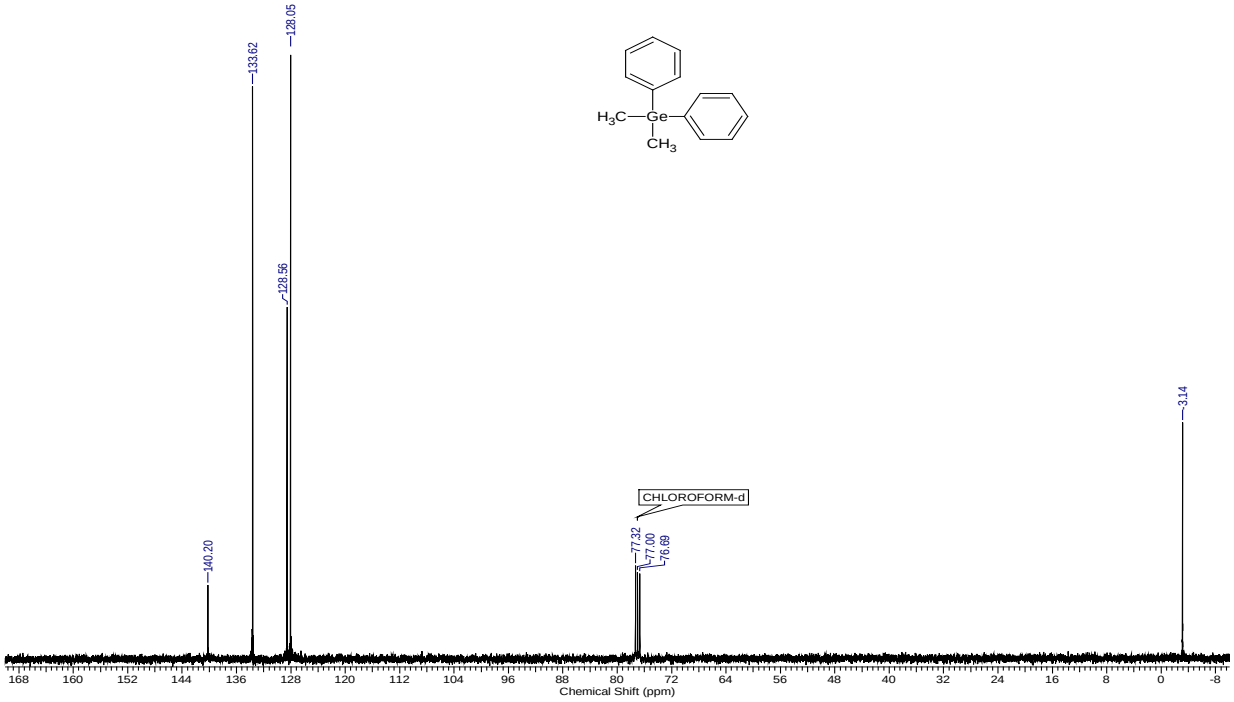


**Figure S2.** $^{13}$C NMR spectrum for $Me_2GePh_2$ ($CDCl_3$, RT).

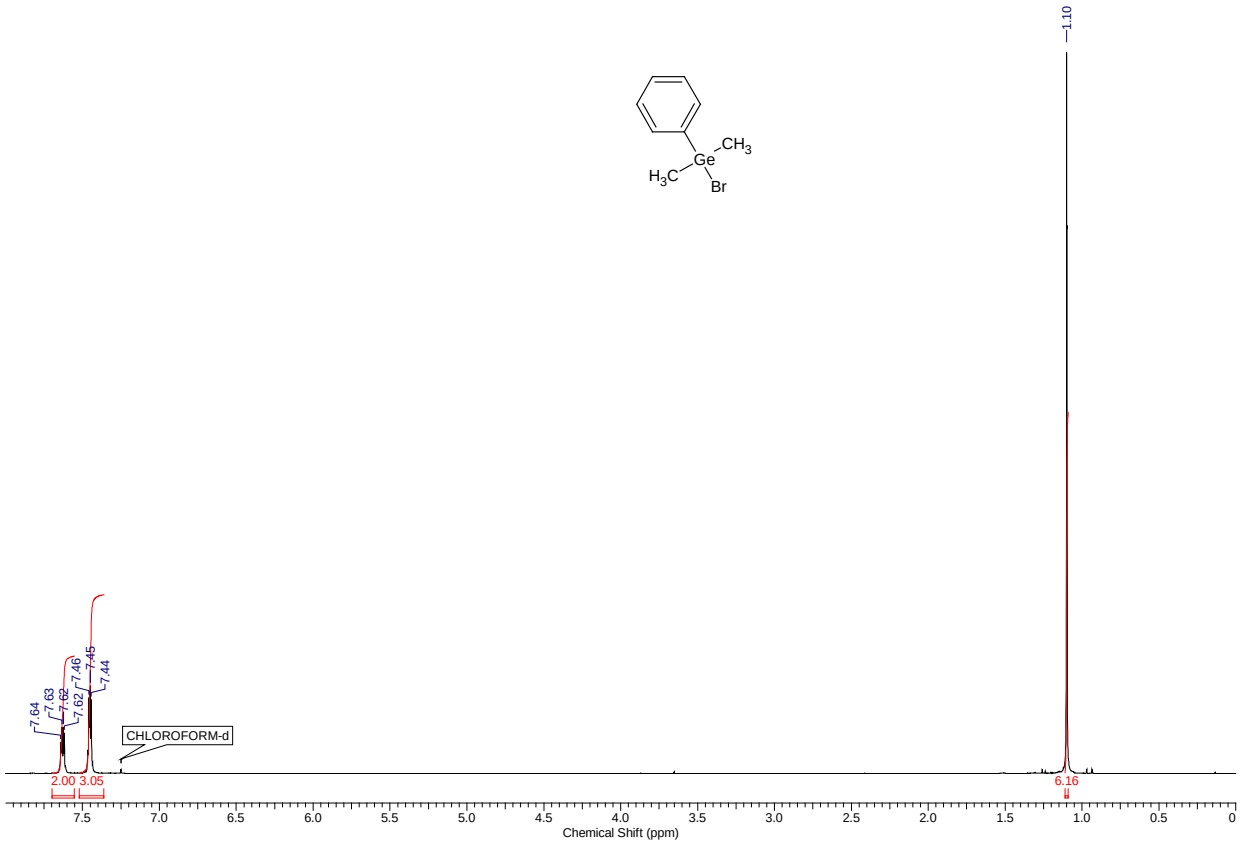


**Figure S3.** $^{1}$H NMR spectrum for $Me_2GePhBr$ ($CDCl_3$, RT).

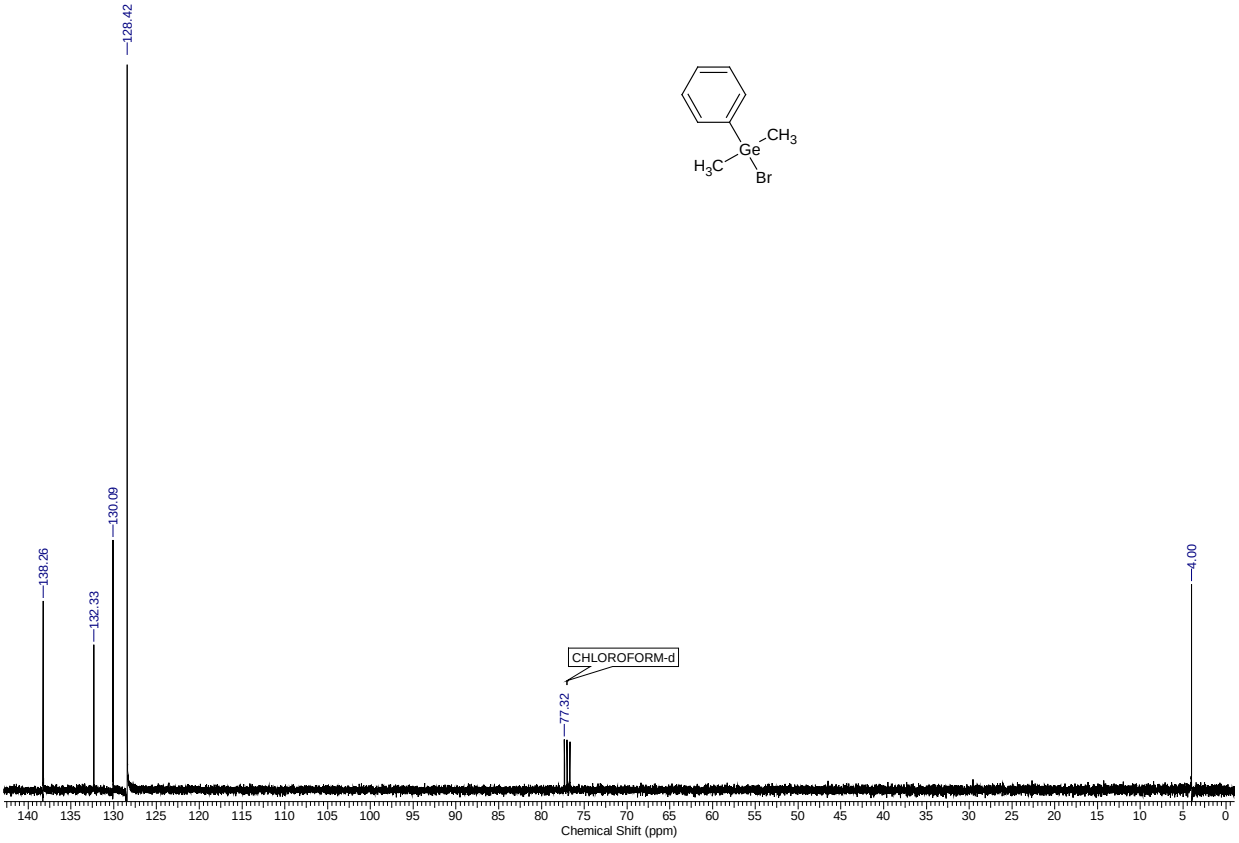


**Figure S4.** $^{13}$C NMR spectrum for $Me_2GePhBr$ ($CDCl_3$, RT).

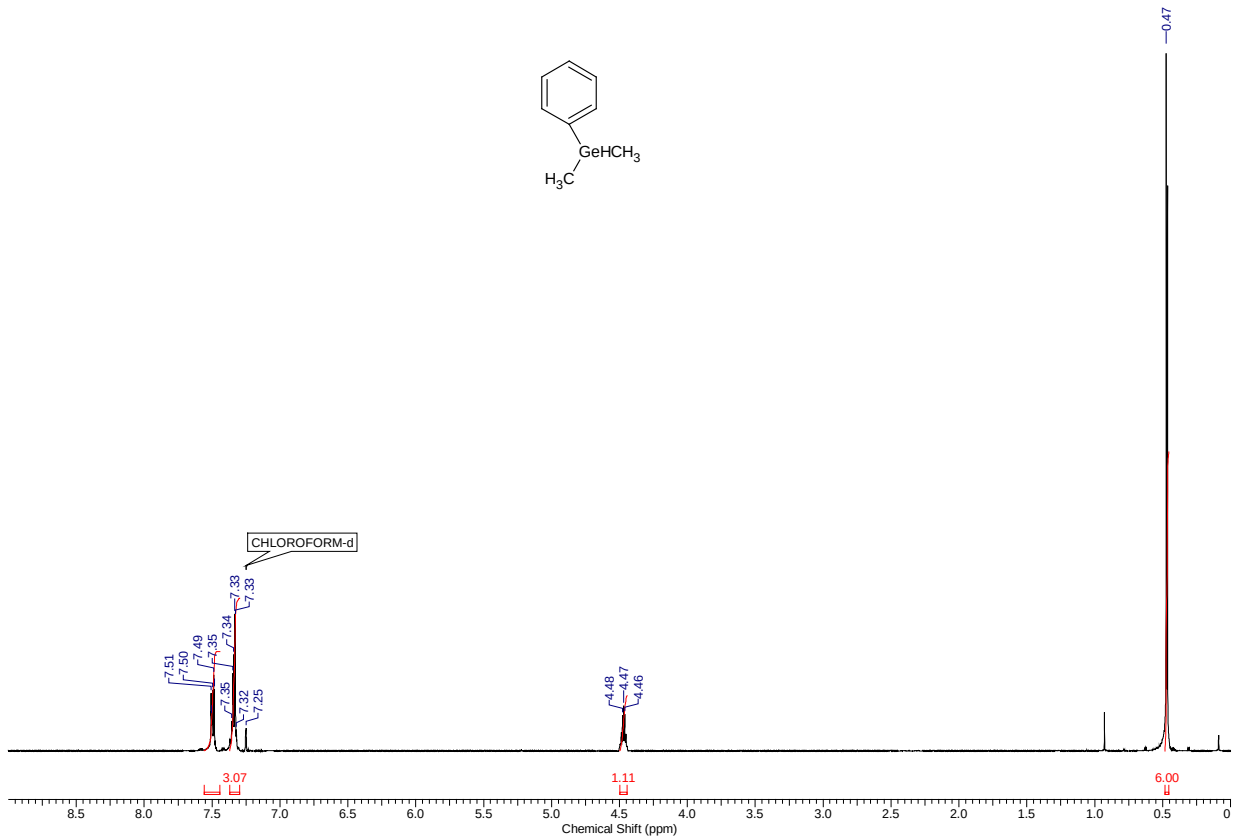


**Figure S5.** $^{1}$H NMR spectrum for $Me_2GePhH$ ($CDCl_3$, RT).

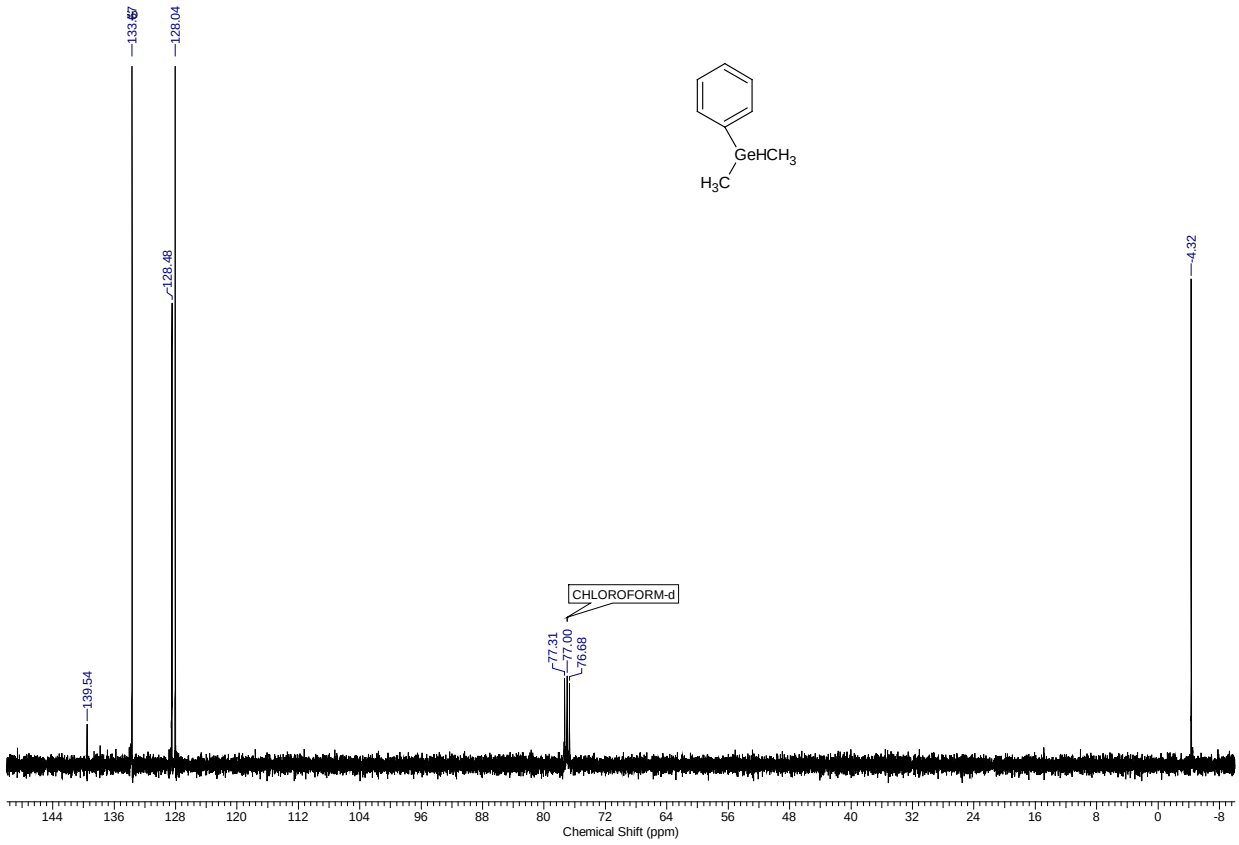


**Figure S6.** $^{13}$C NMR spectrum for $Me_2GePhH$ ($CDCl_3$, RT).

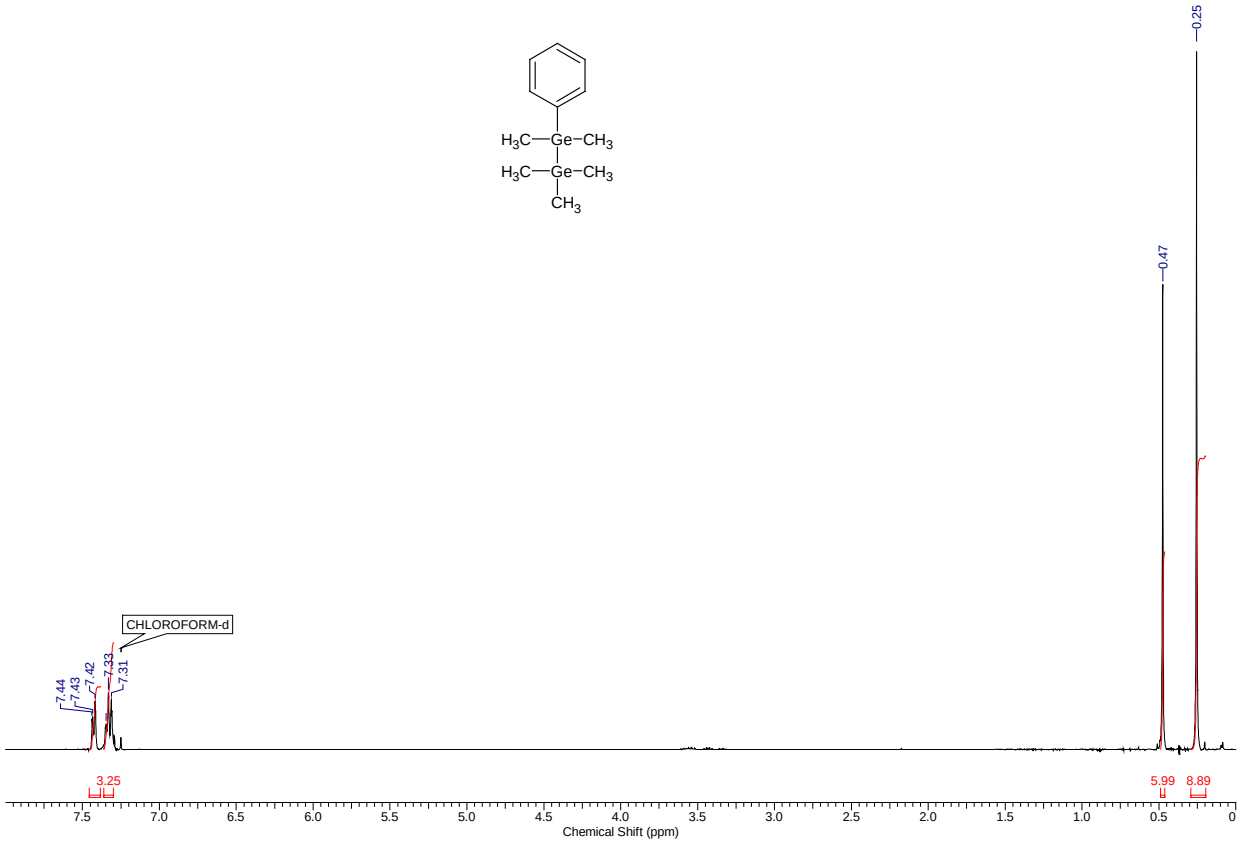


**Figure S7.** $^{1}$H NMR spectrum for $PhMe_2GeGeMe_3$ ($CDCl_3$, RT).

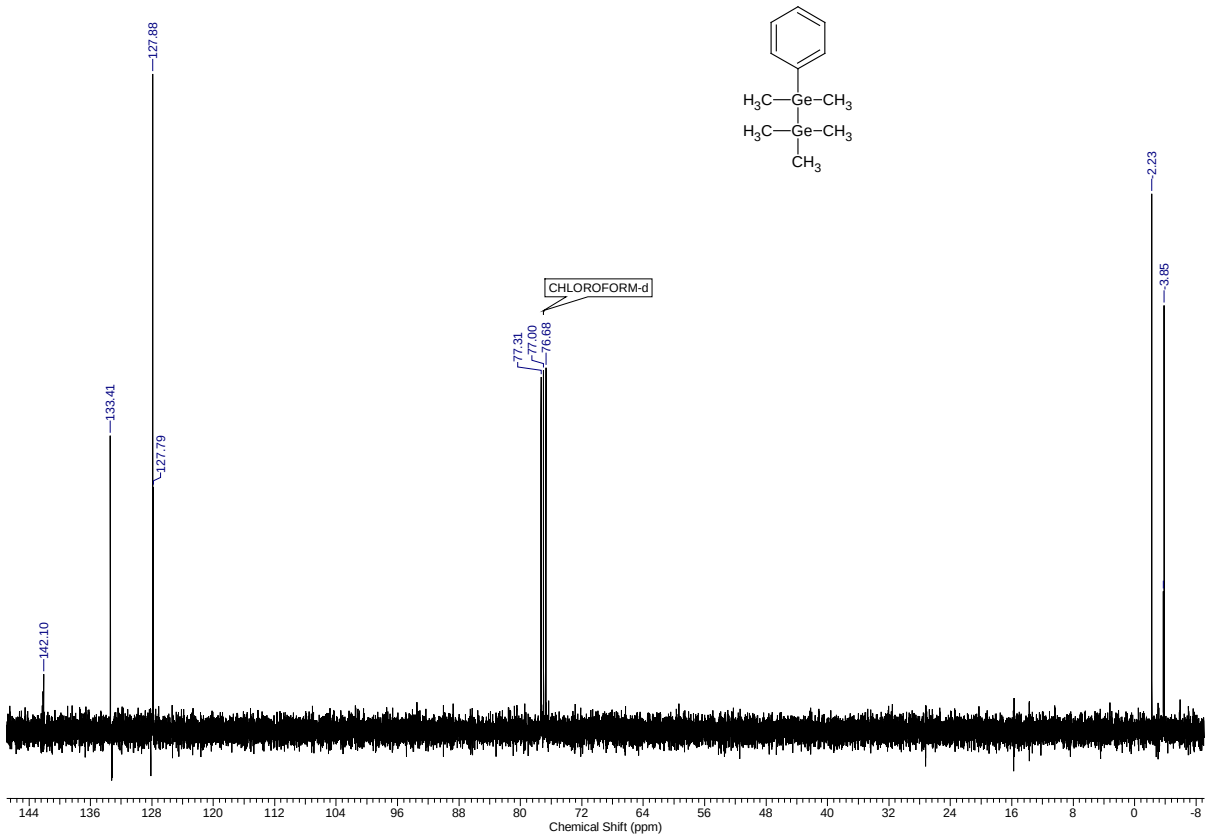


**Figure S8.** $^{13}$C NMR spectrum for $PhMe_2GeGeMe_3$ ($CDCl_3$, RT).

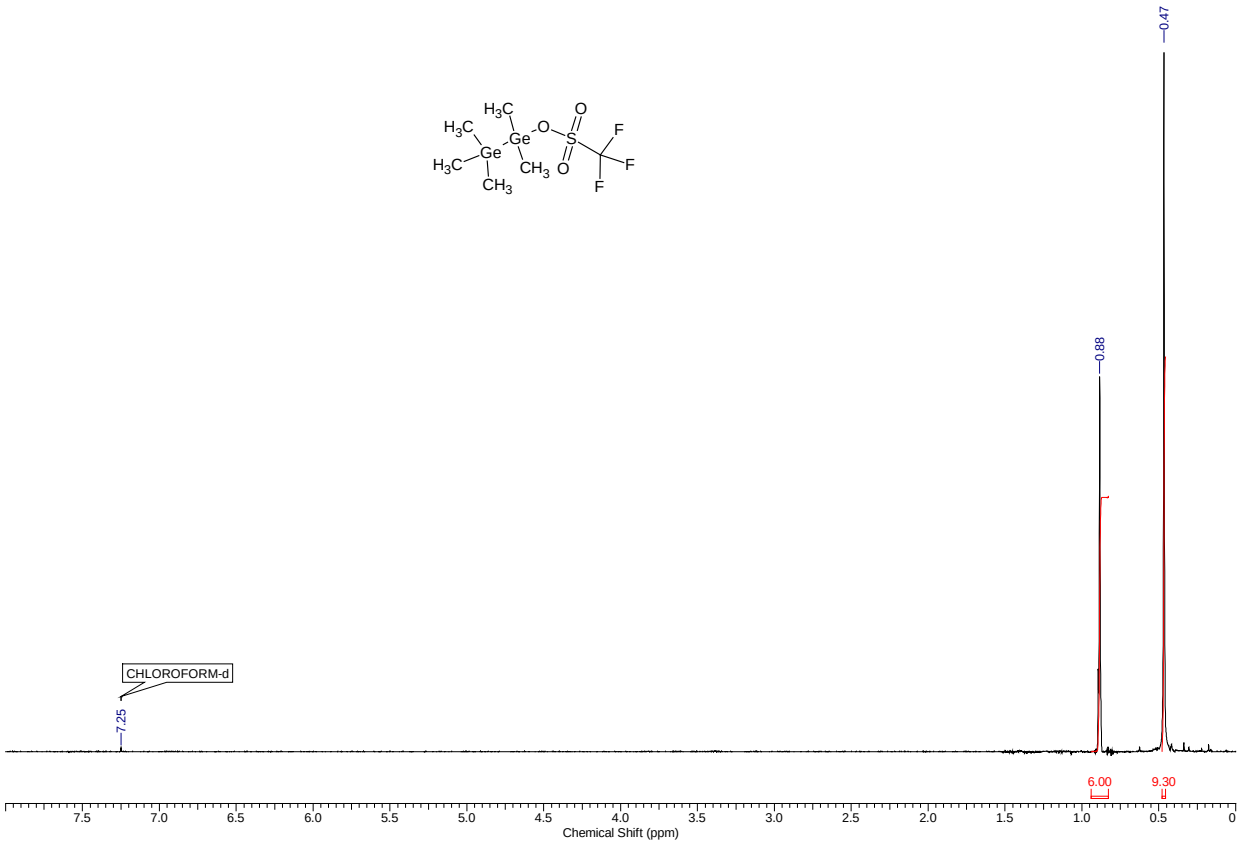


**Figure S9.** $^{1}$H NMR spectrum for $Me_3GeGeMe_2OTf$ ($CDCl_3$, RT).

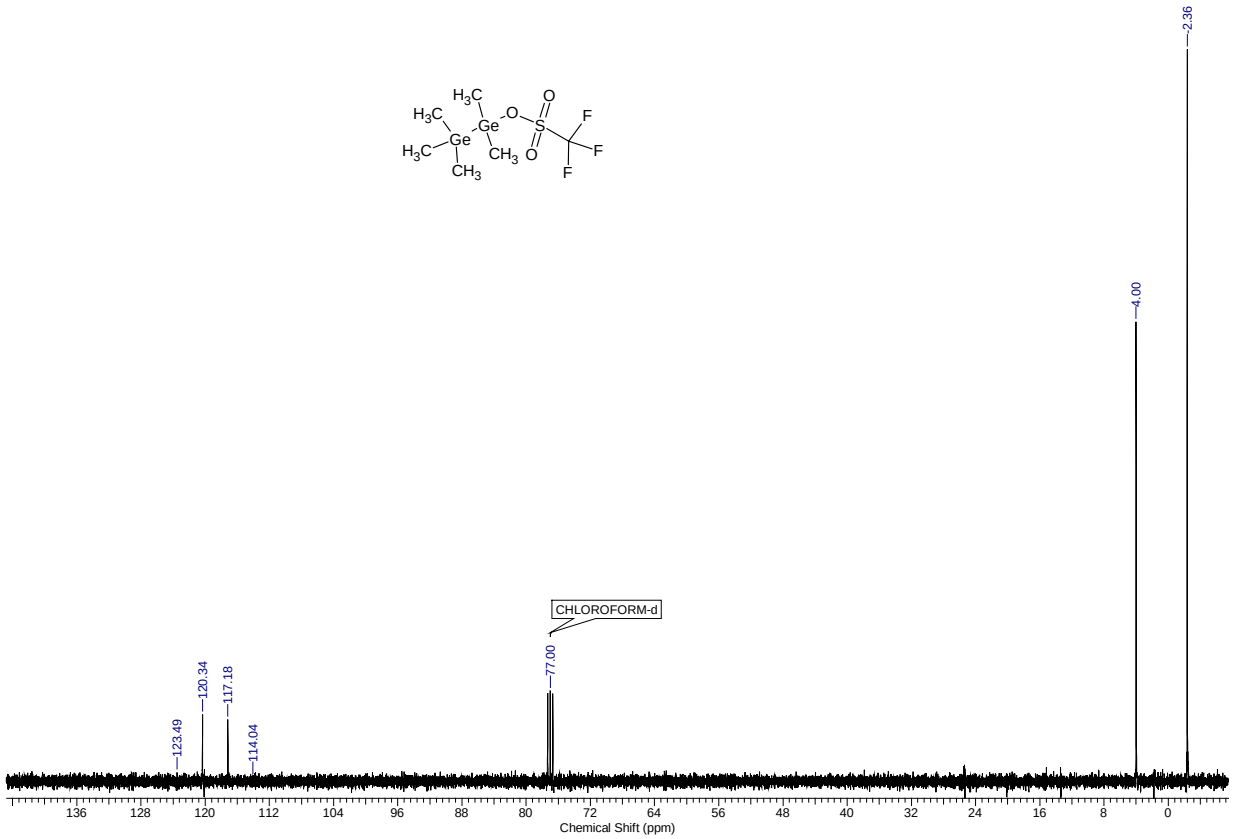


**Figure S10.** $^{13}$C NMR spectrum for $Me_3GeGeMe_2OTf$ ($CDCl_3$, RT).

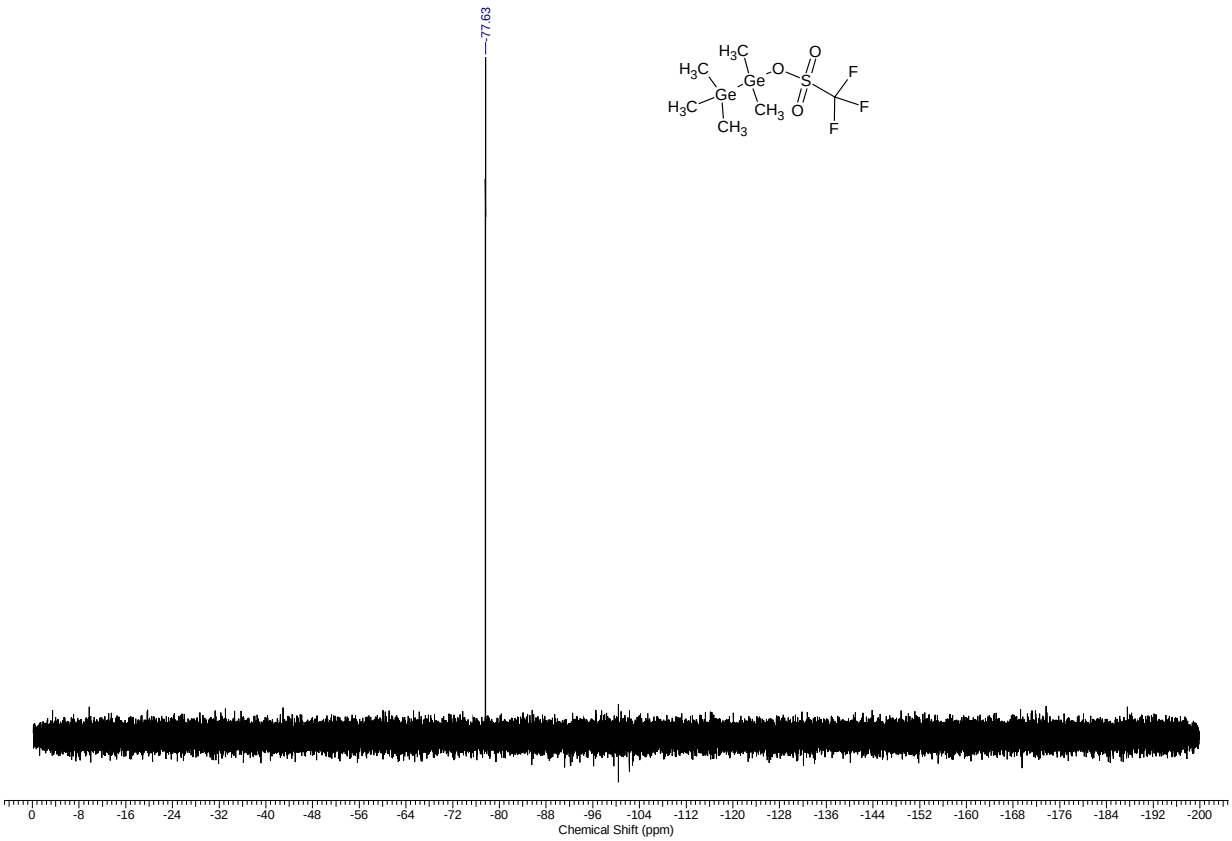


**Figure S11.** $^{19}$F NMR spectrum for $Me_3GeGeMe_2OTf$ ($CDCl_3$, RT).

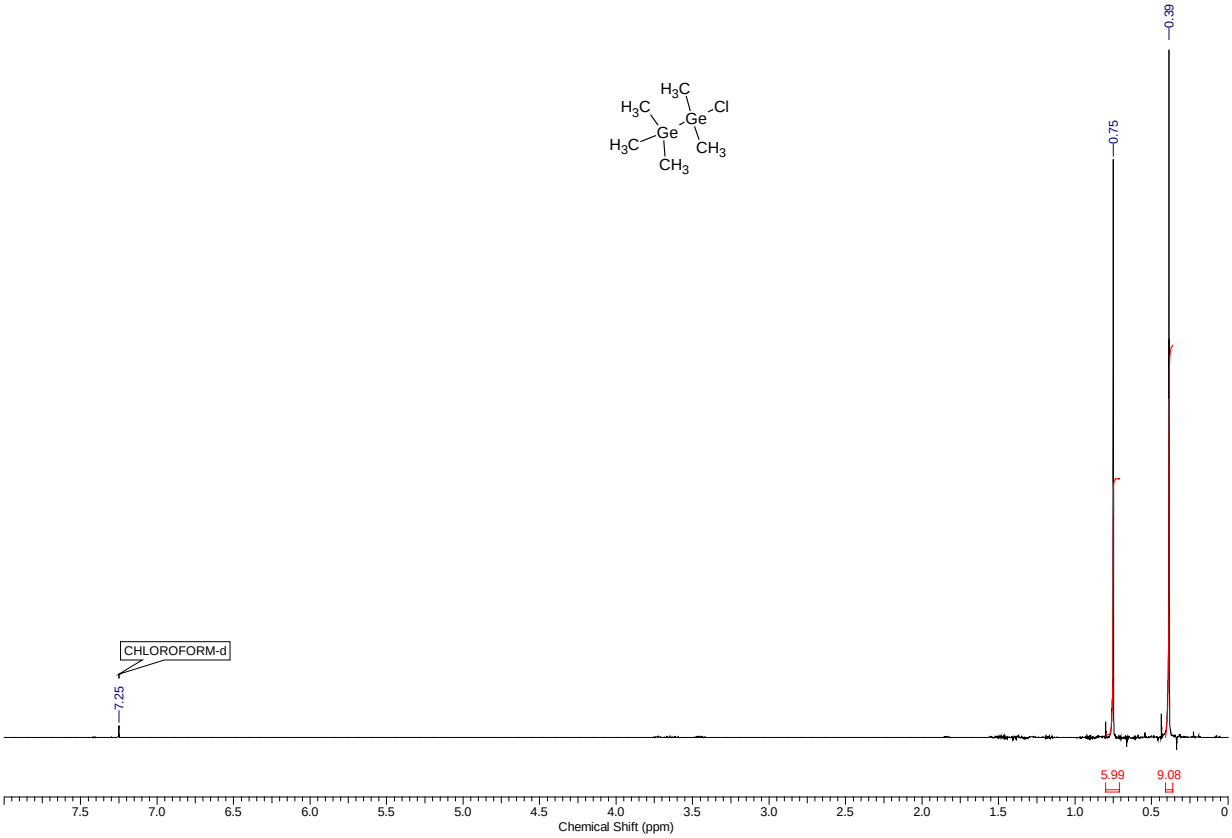


**Figure S12.** $^{1}$H NMR spectrum for $Me_3GeGeMe_2Cl$ ($CDCl_3$, RT).

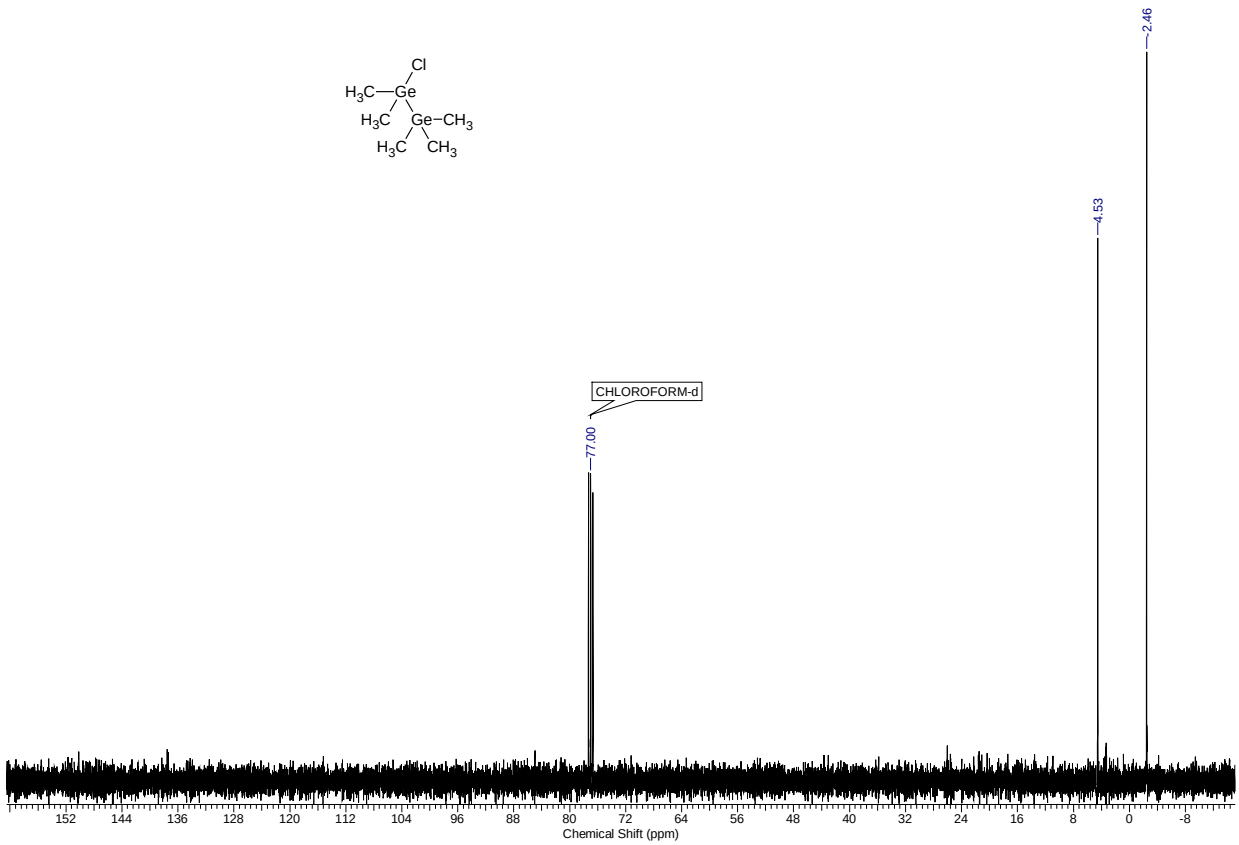


**Figure S13.** $^{13}C$ NMR spectrum for $Me_3GeGeMe_2Cl$ ($CDCl_3$, RT).

## NMR spectra of oligothienyl catenated Group 14 derivatives

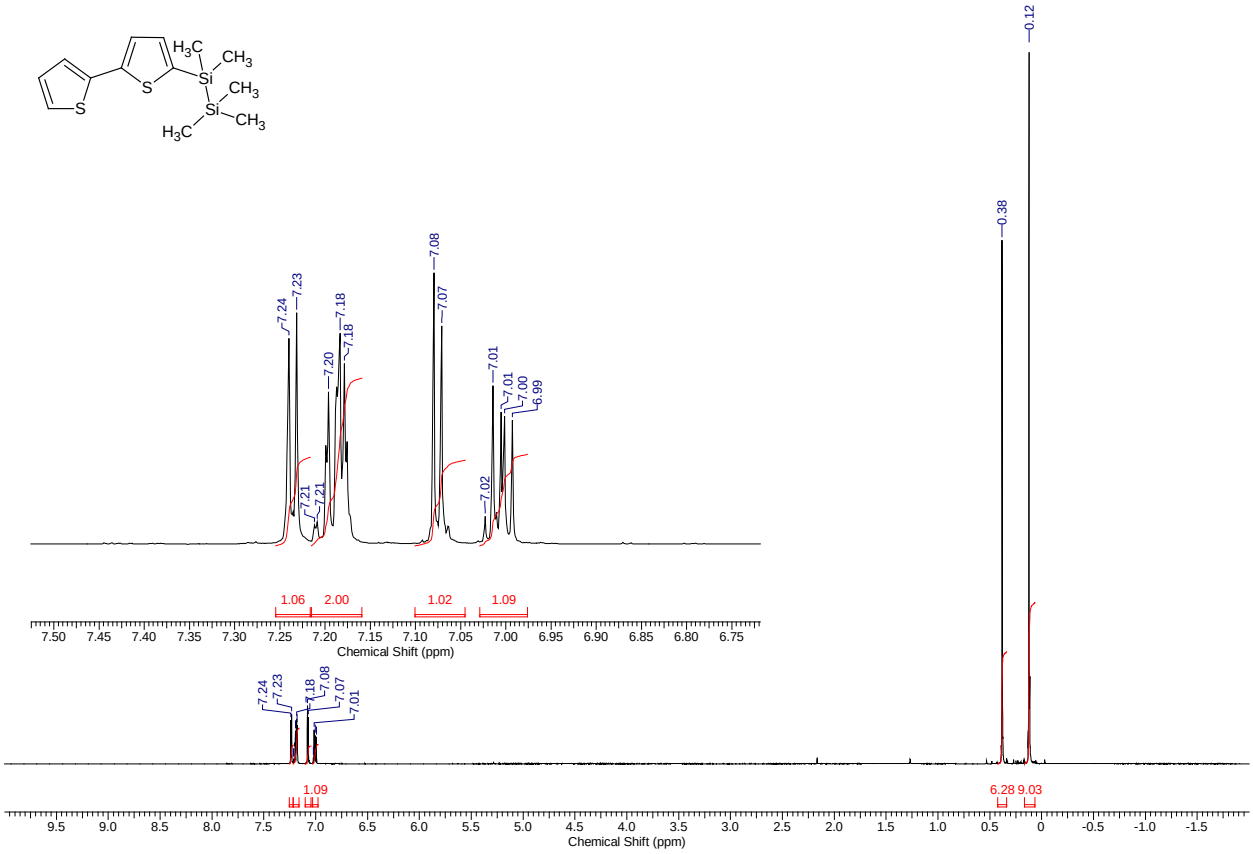


**Figure S14.** $^{1}$H NMR spectrum for **1a** ($CDCl_3$, RT).

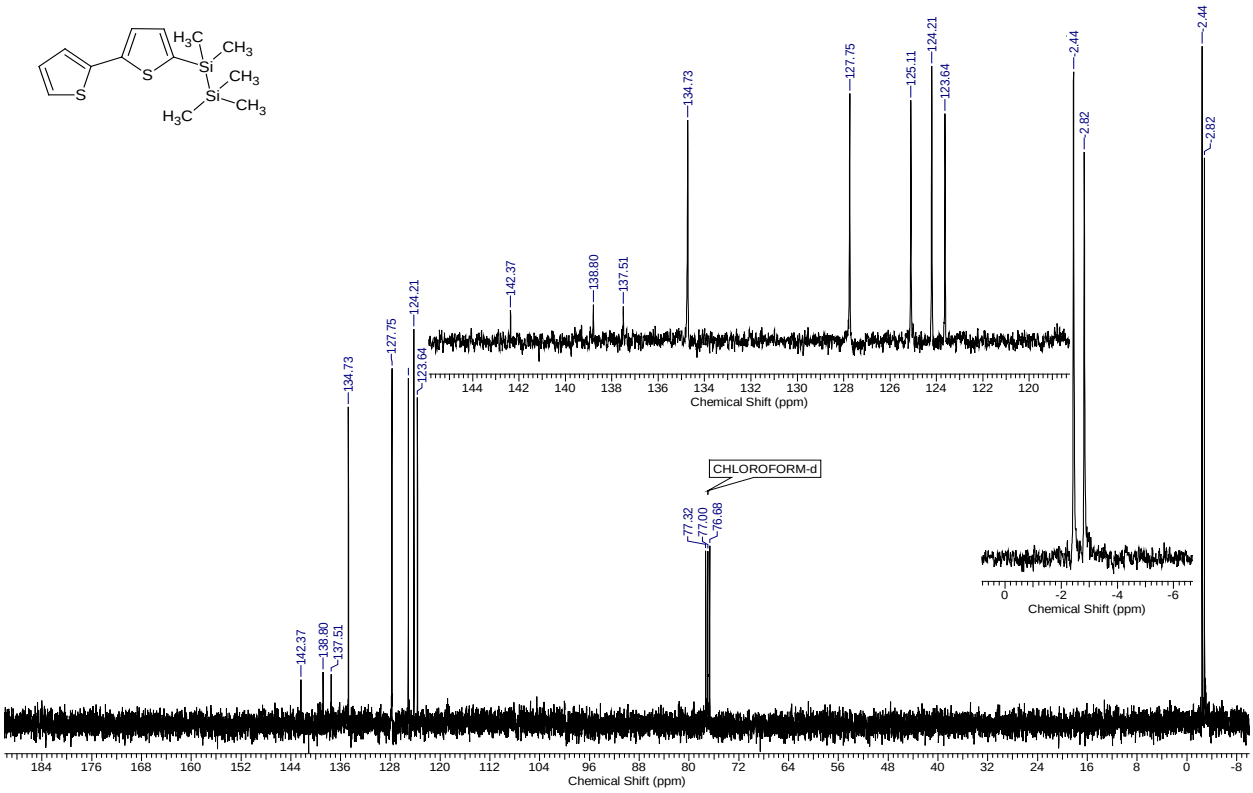


**Figure S15.** $^{13}$C NMR spectrum for **1a** ($CDCl_3$, RT).

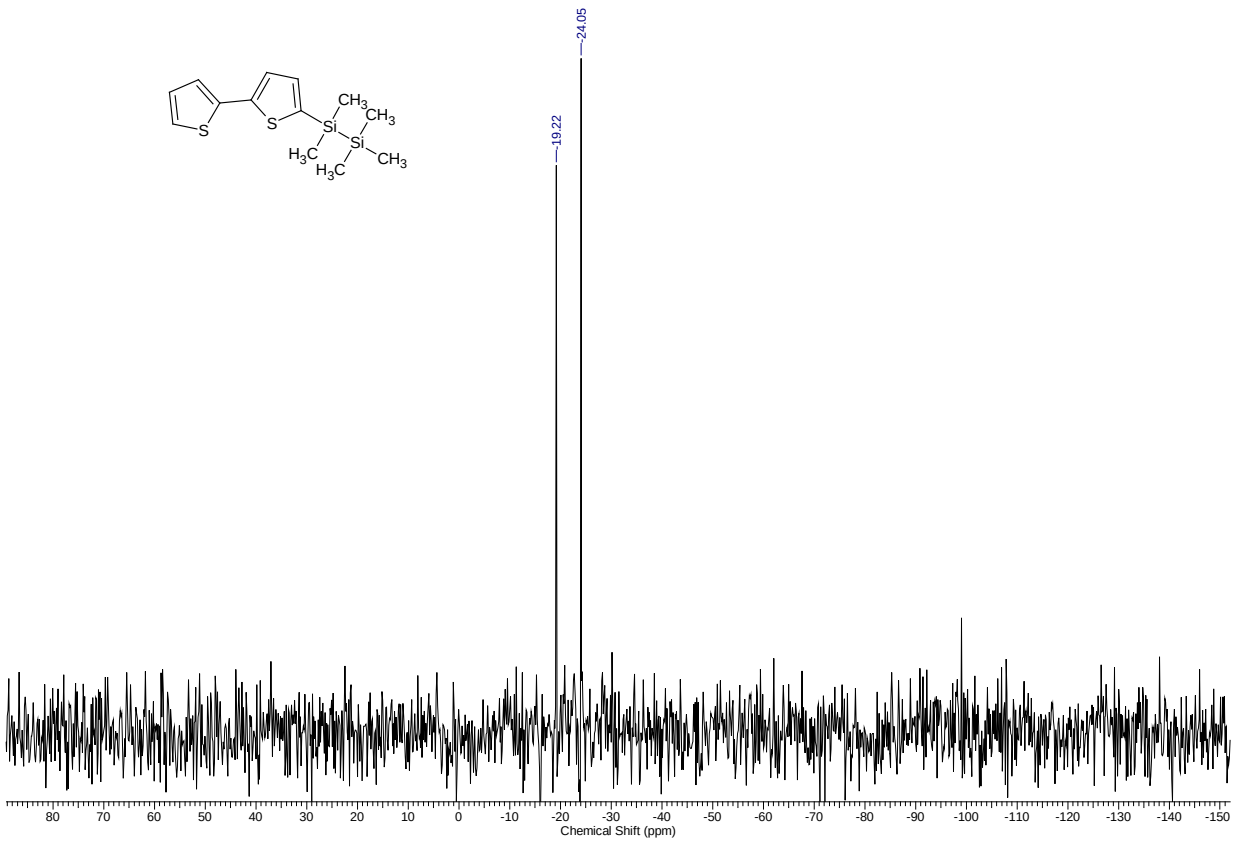


**Figure S16.** $^{29}$Si NMR spectrum for **1a** ($CDCl_3$, RT).

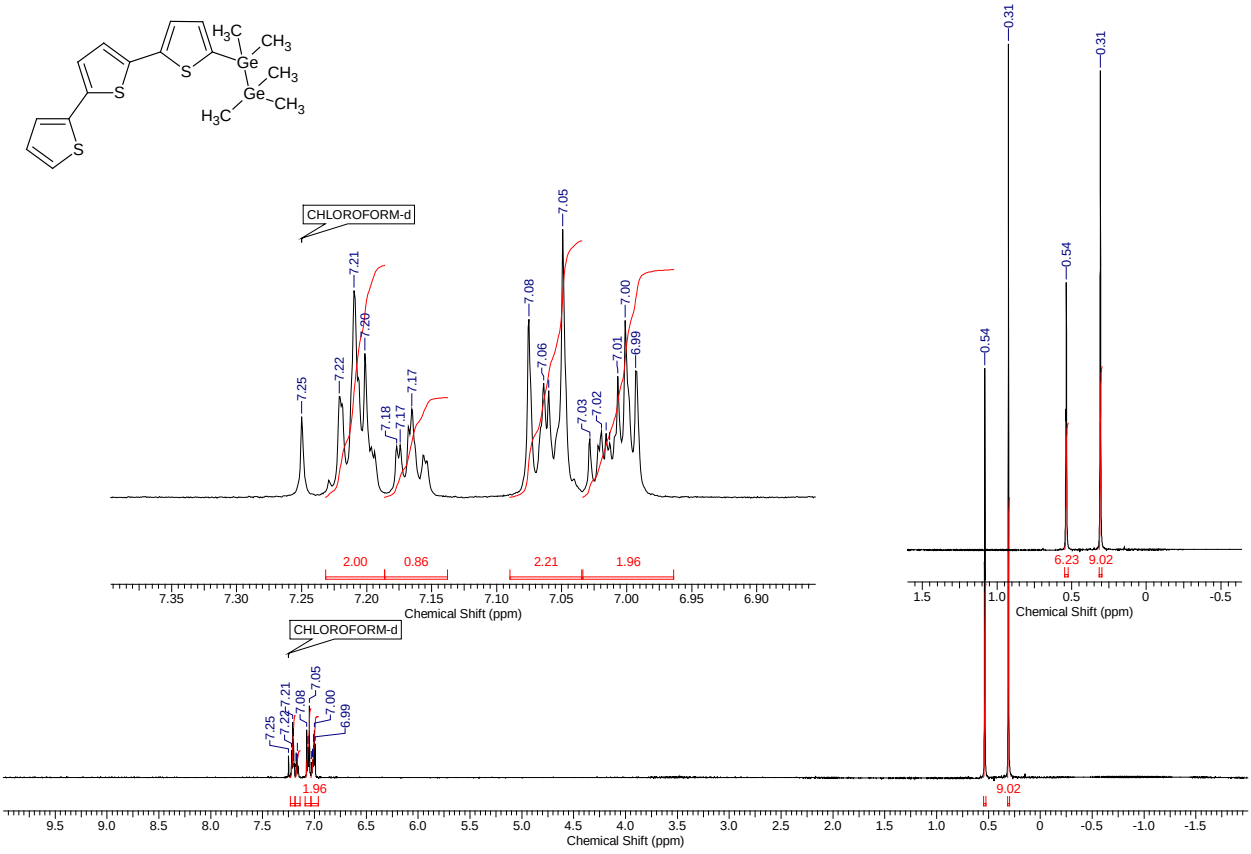


**Figure S17.** $^{1}$H NMR spectrum for **1b** ($CDCl_3$, RT).

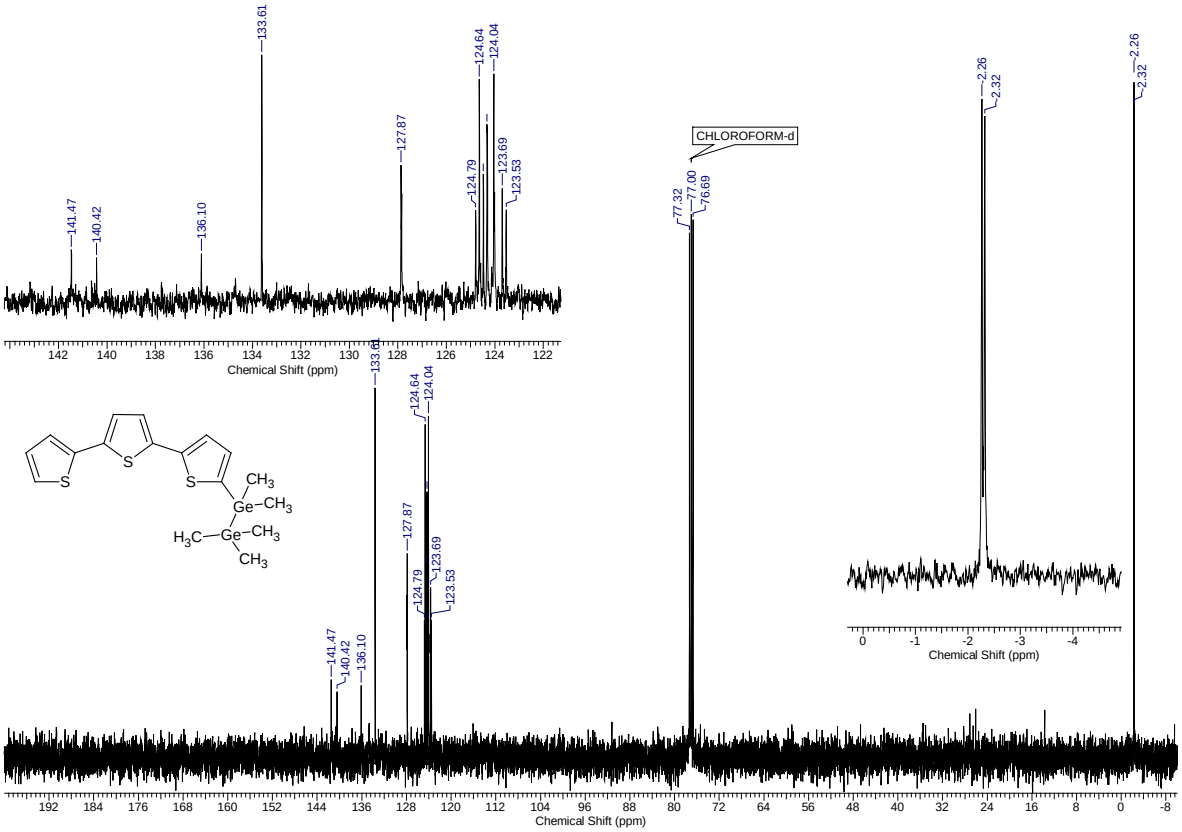


**Figure S18.** $^{13}$C NMR spectrum for **1b** ($CDCl_3$, RT).

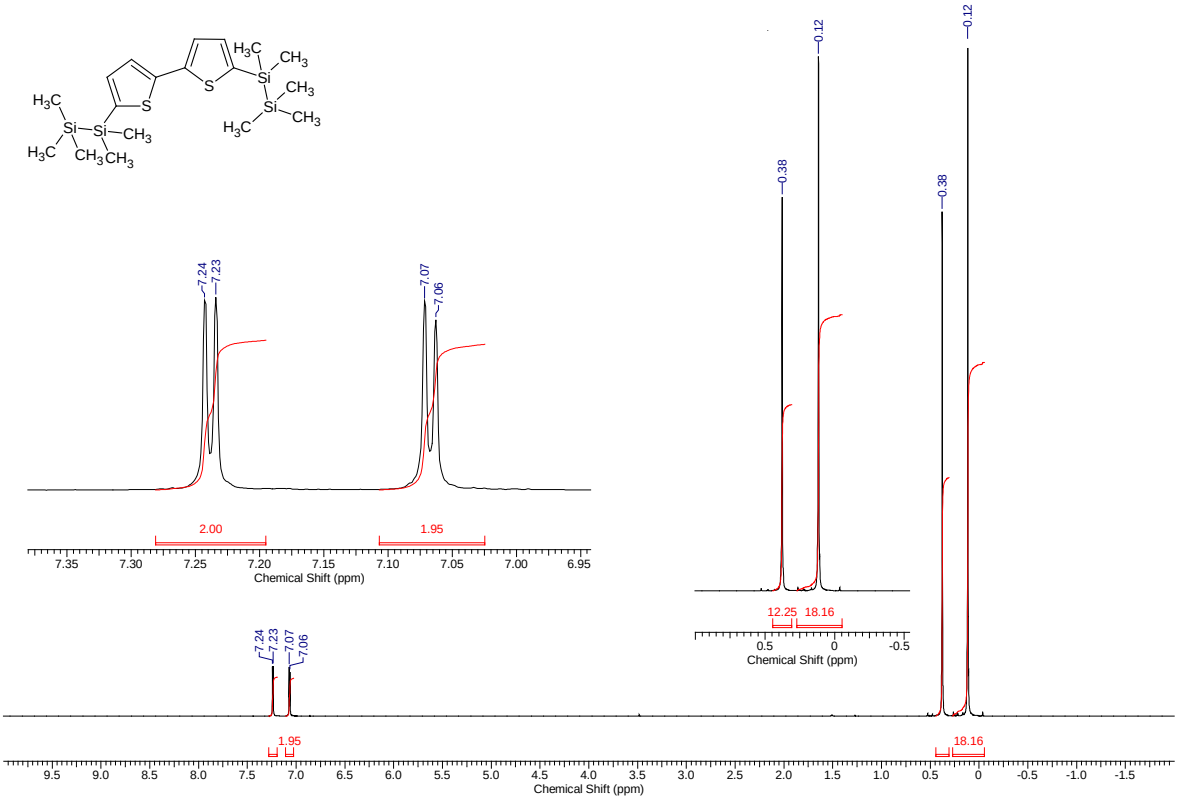


**Figure S19.** $^{1}$H NMR spectrum for **2a** ($CDCl_3$, RT).

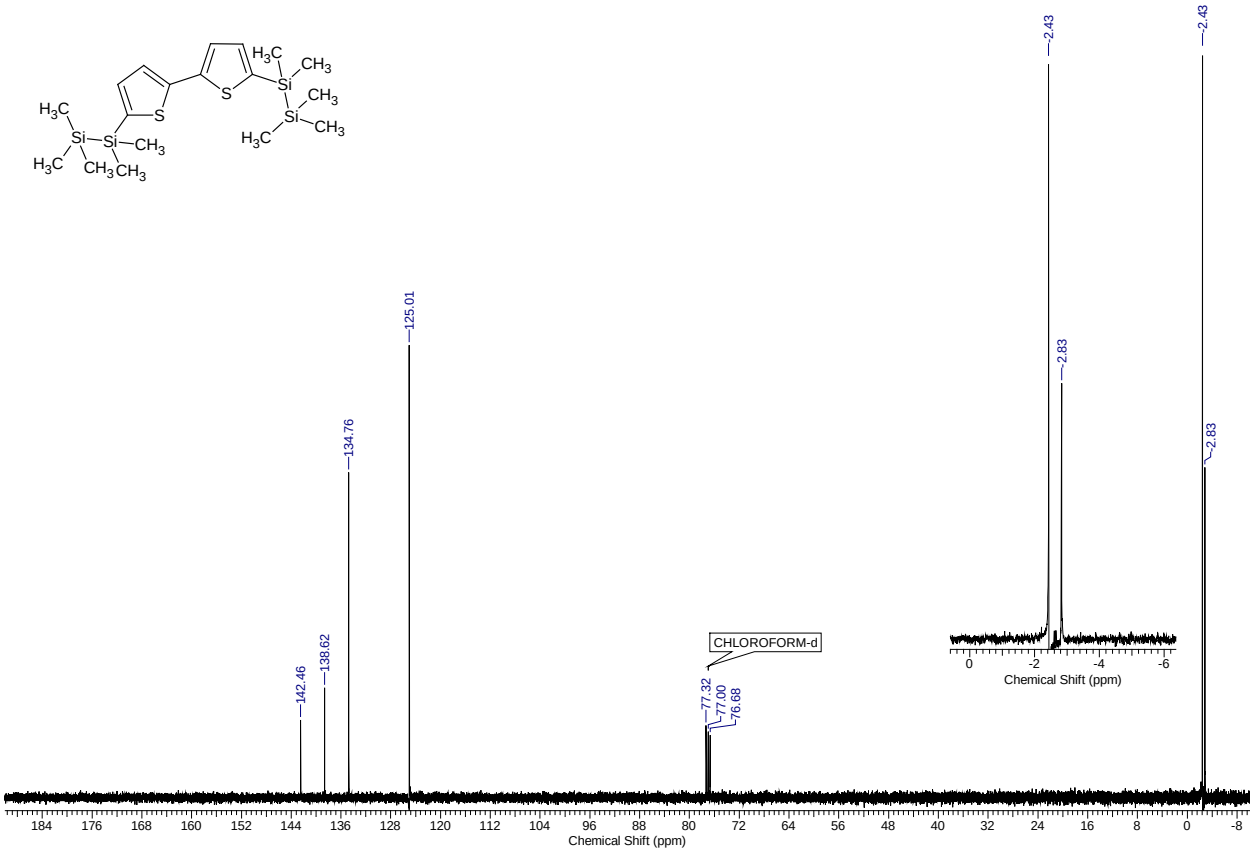


**Figure S20.** $^{13}$C NMR spectrum for **2a** ($CDCl_3$, RT).

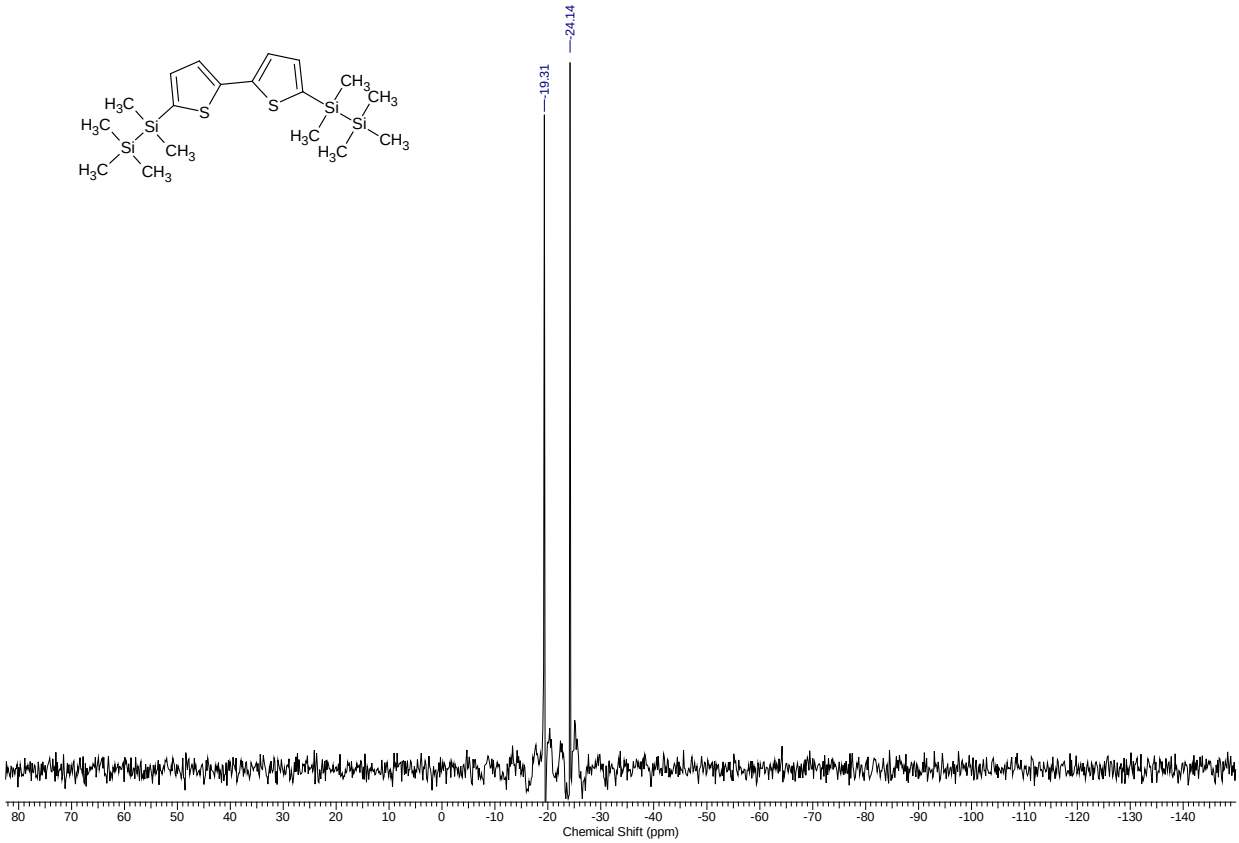


**Figure S21.** $^{29}$Si NMR spectrum for **2a** ($CDCl_3$, RT).

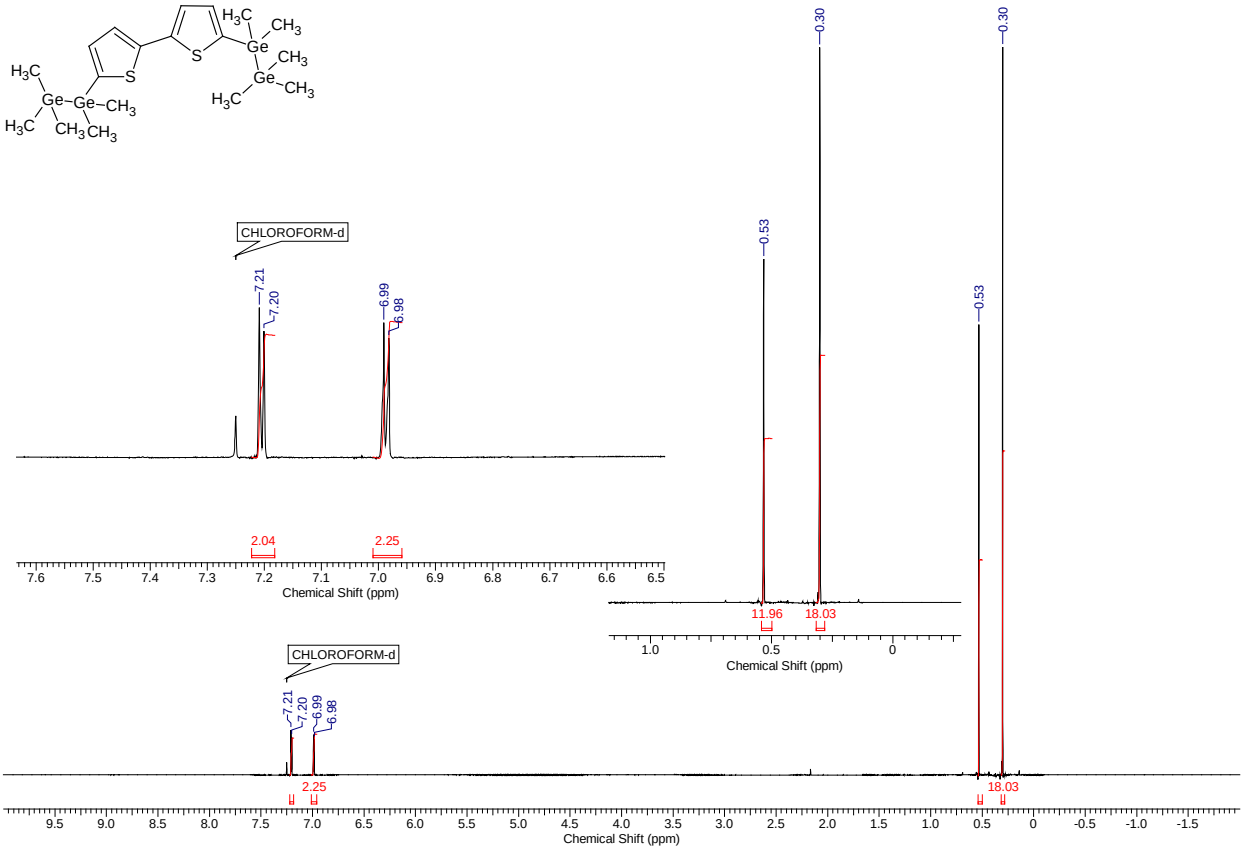


**Figure S22.** $^{1}$H NMR spectrum for **2b** ($CDCl_3$, RT).

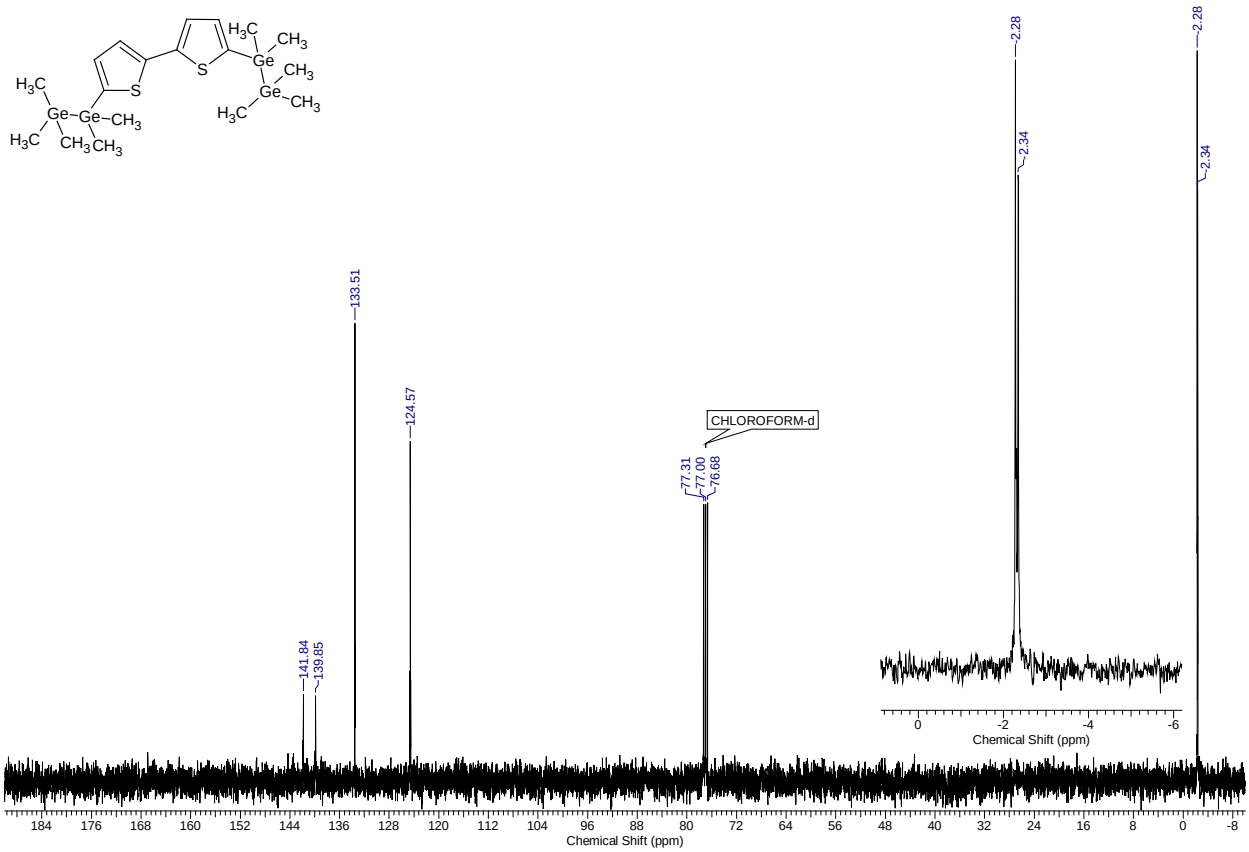


**Figure S23.** $^{13}$C NMR spectrum for **2b** ($CDCl_3$, RT).

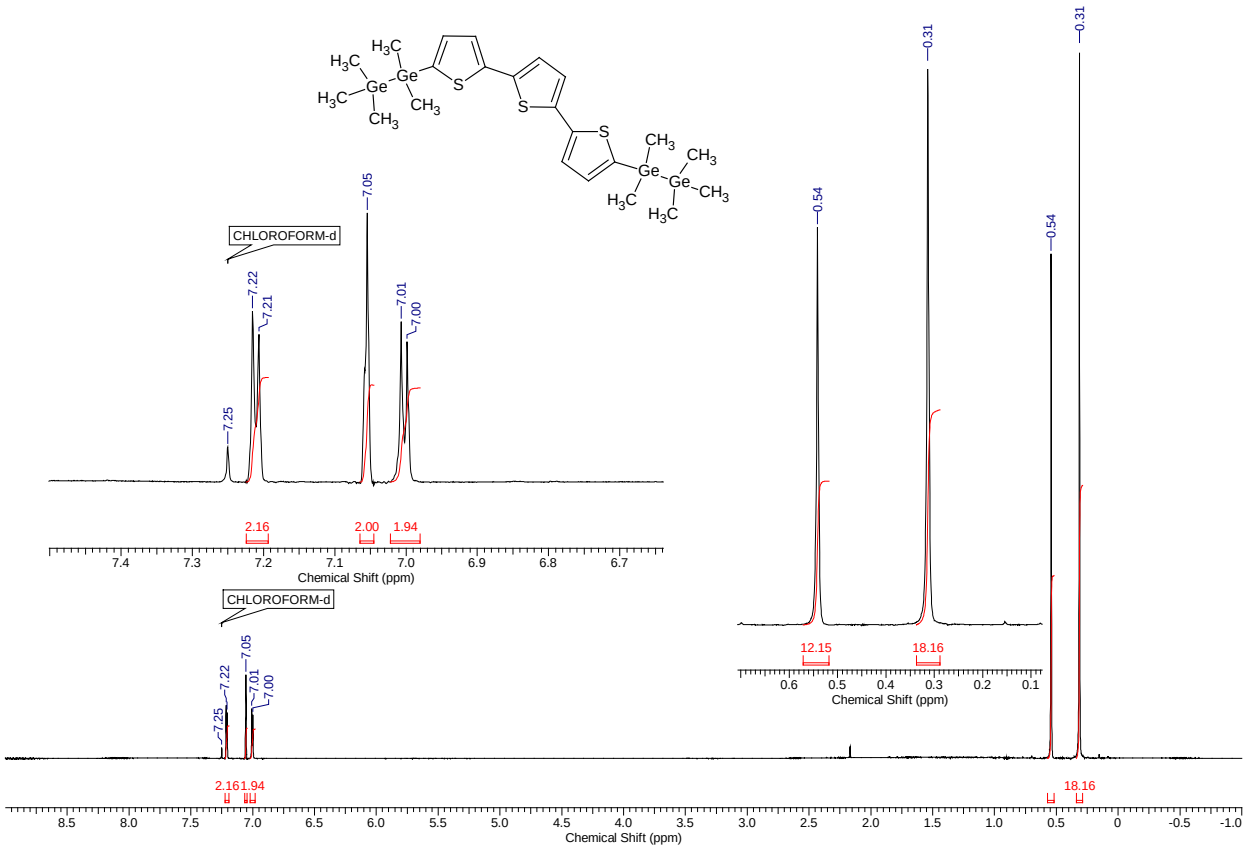


**Figure S24.** $^{1}$H NMR spectrum for **2c** ($CDCl_3$, RT).

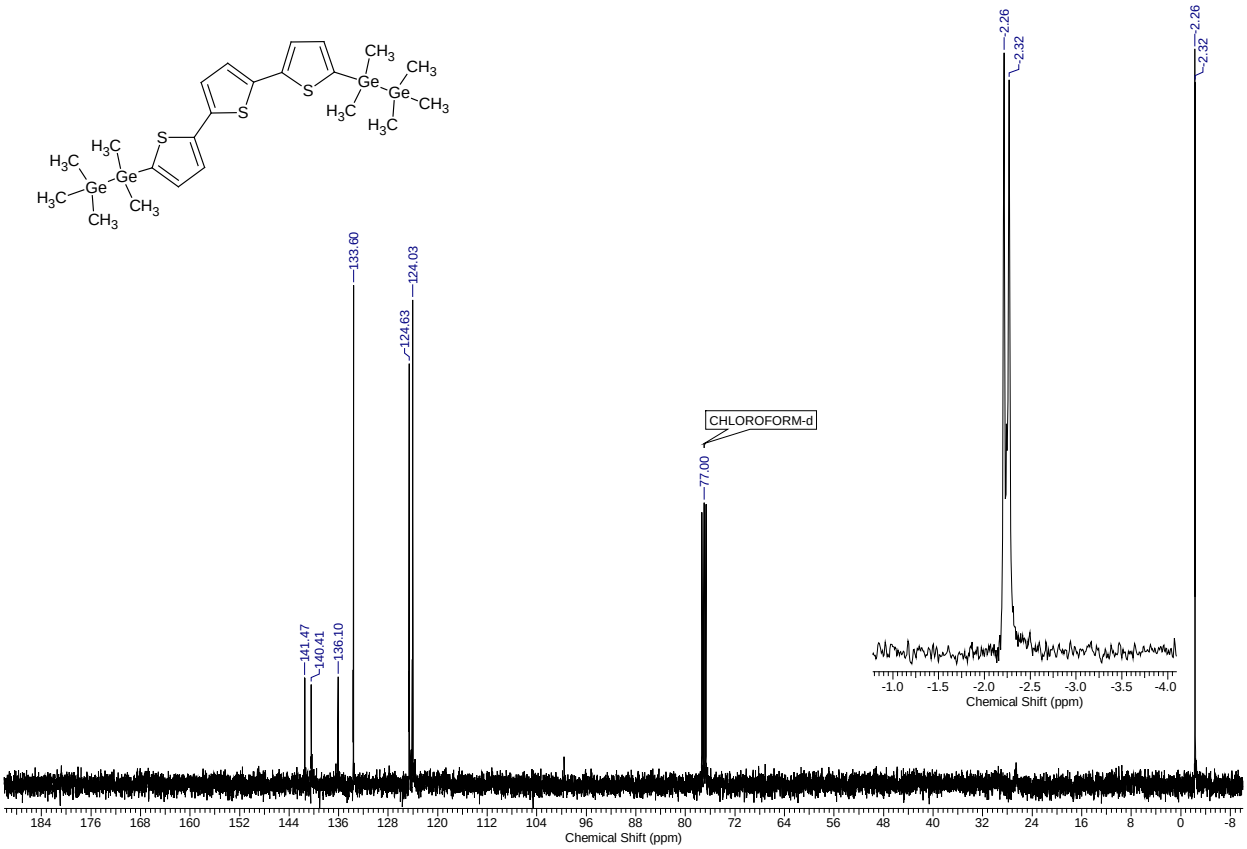


**Figure S25.** $^{13}$C NMR spectrum for **2c** ($CDCl_3$, RT).

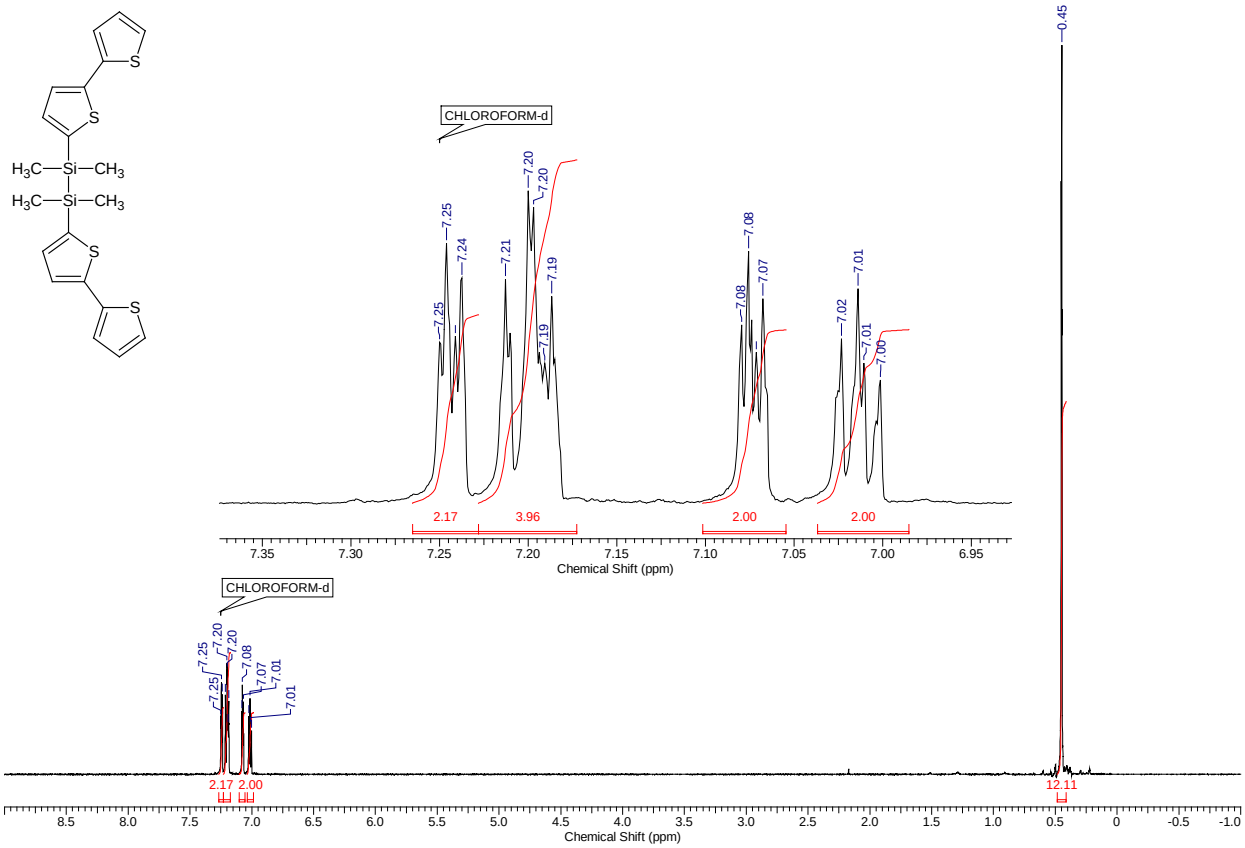


**Figure S26.** $^{1}$H NMR spectrum for **3a** ($CDCl_3$, RT).

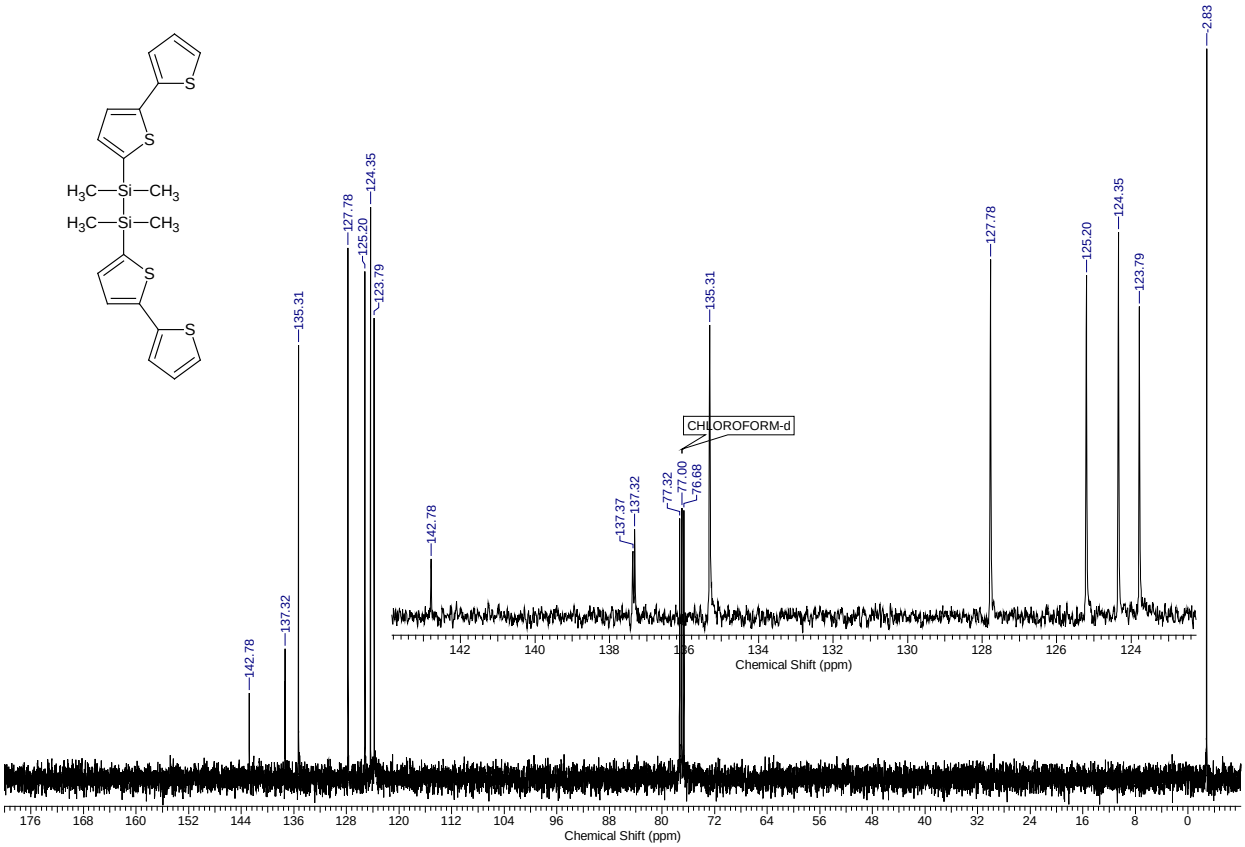


**Figure S27.** $^{13}$C NMR spectrum for **3a** ($CDCl_3$, RT).

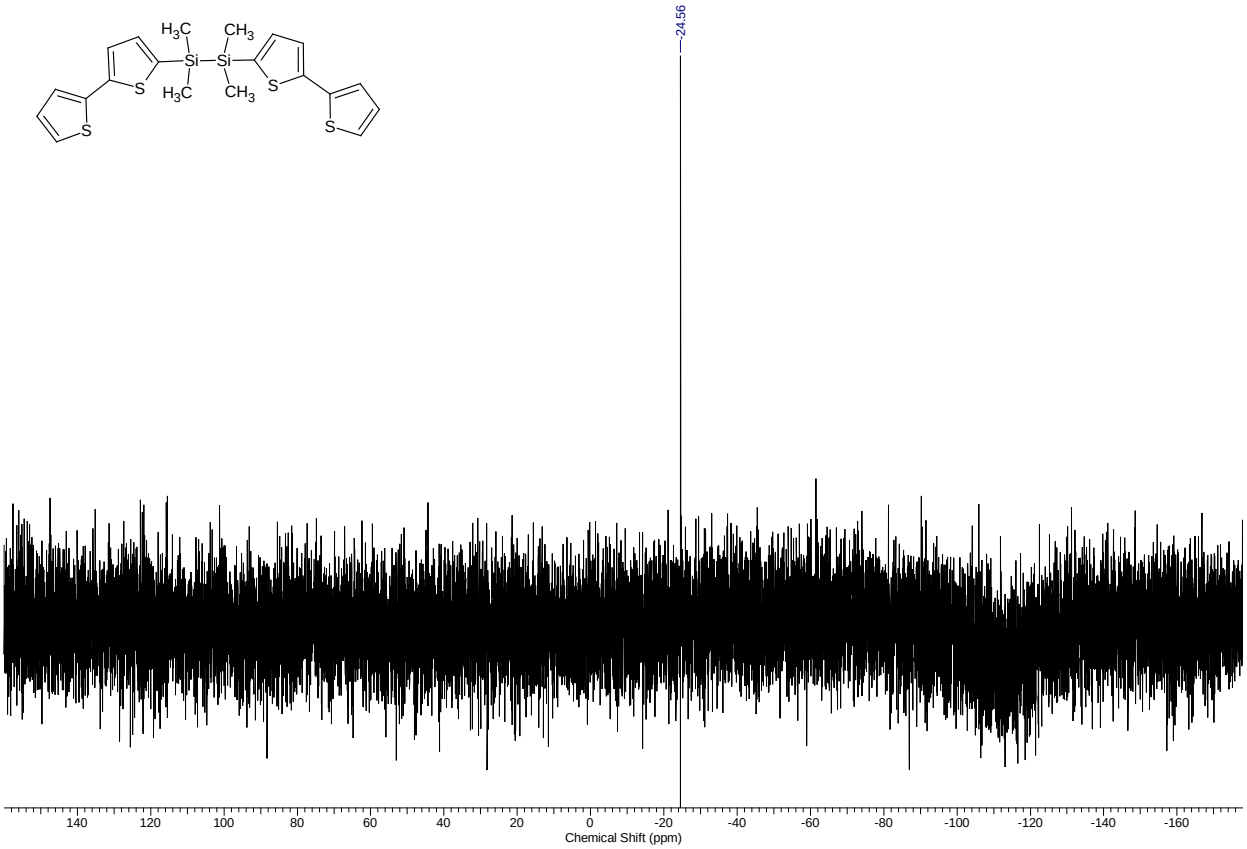


**Figure S28.** $^{29}$Si NMR spectrum for **3a** ($CDCl_3$, RT).

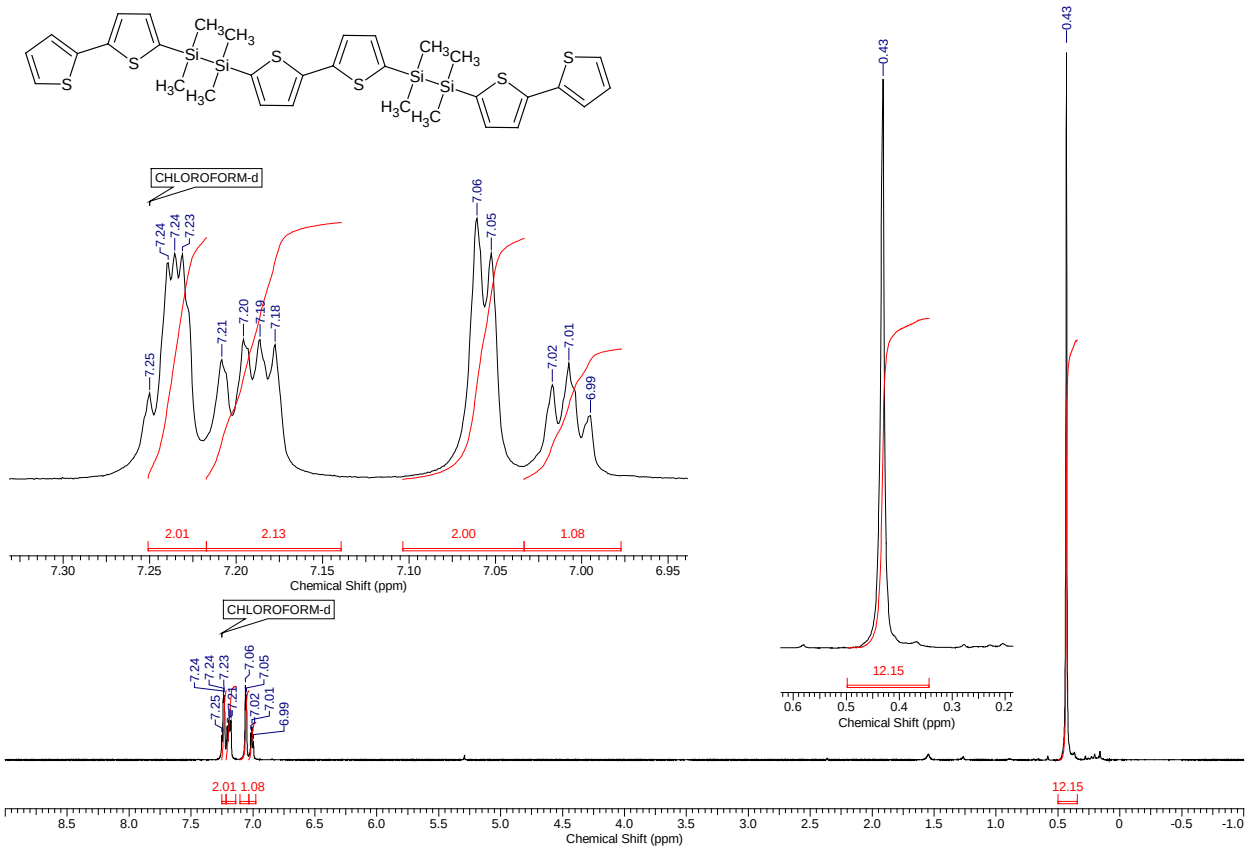


**Figure S29.** $^{1}$H NMR spectrum for **3a'** ($CDCl_3$, RT).

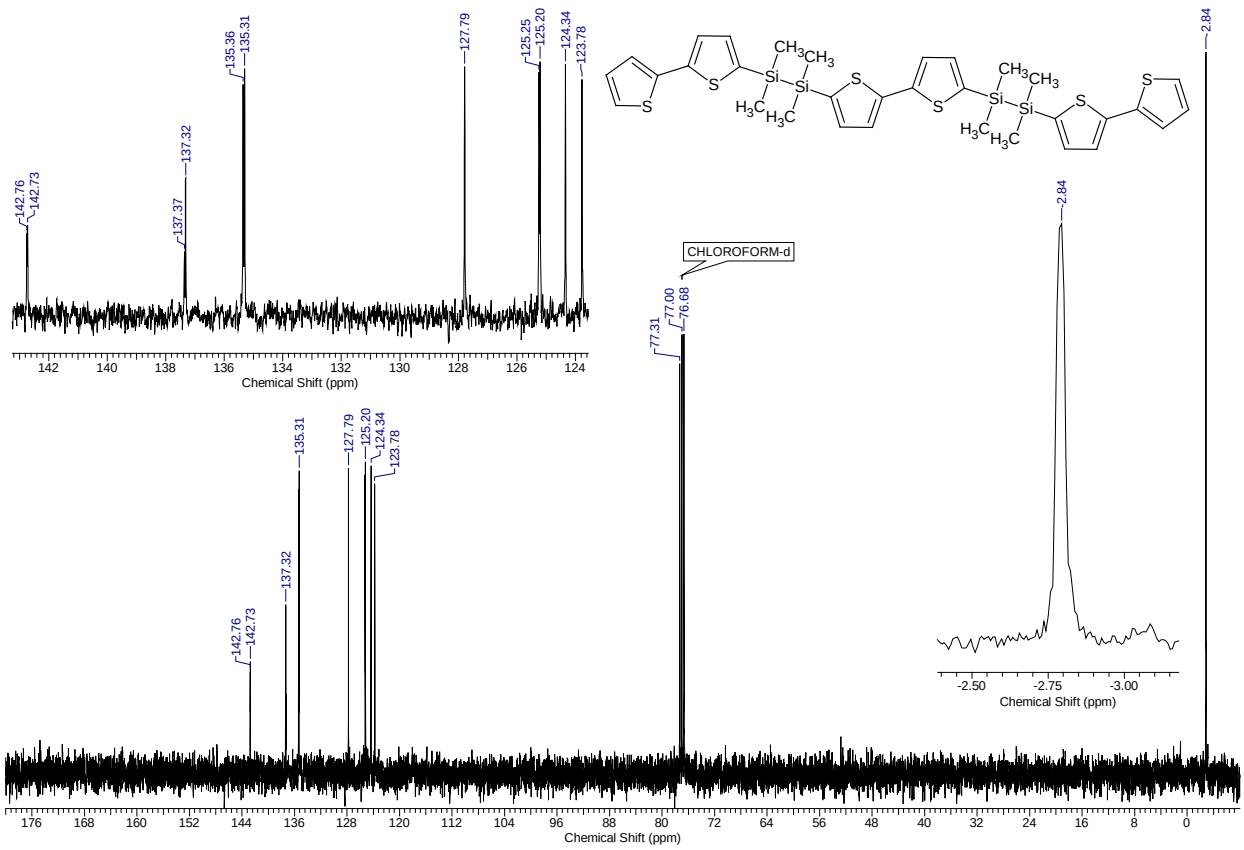


**Figure S30.** $^{13}$C NMR spectrum for **3a'** ($CDCl_3$, RT).

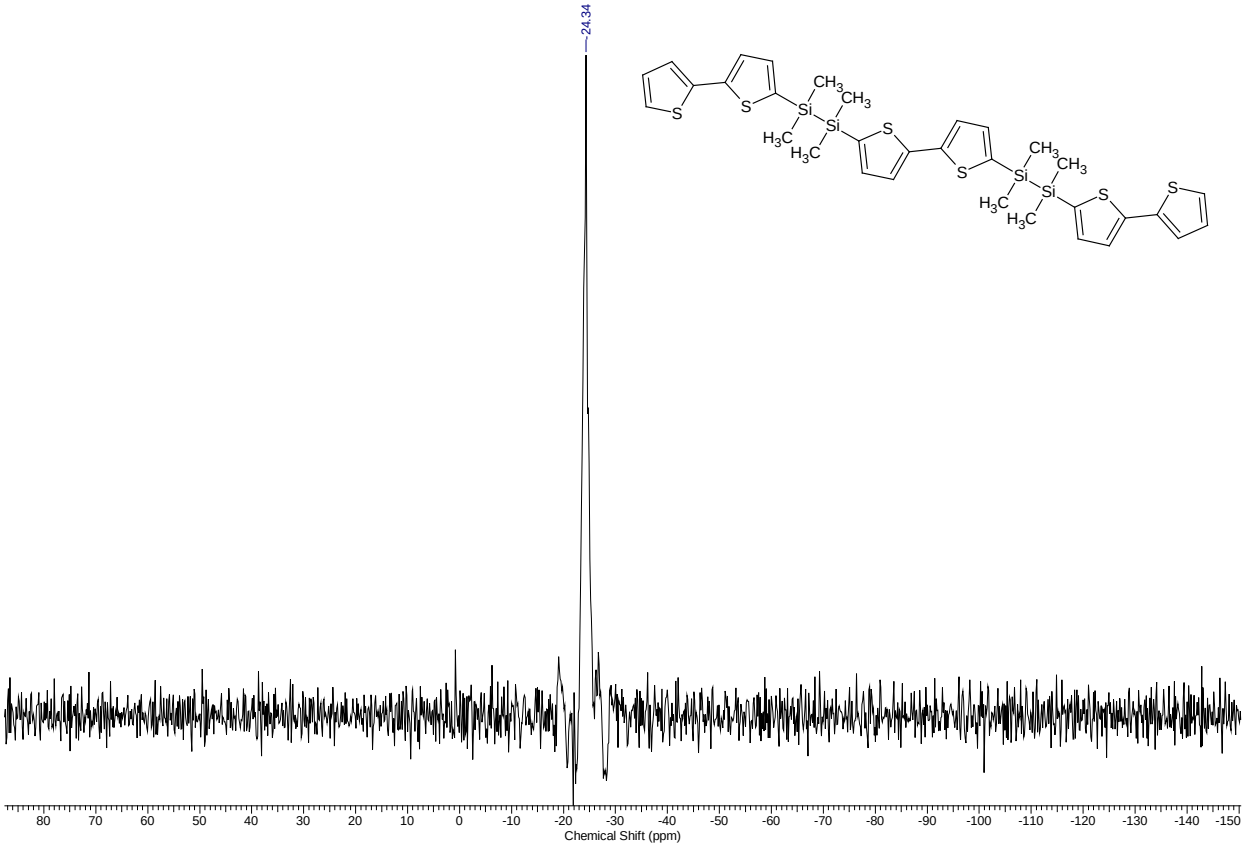


**Figure S31.** $^{29}$Si NMR spectrum for **3a'** ($CDCl_3$, RT).

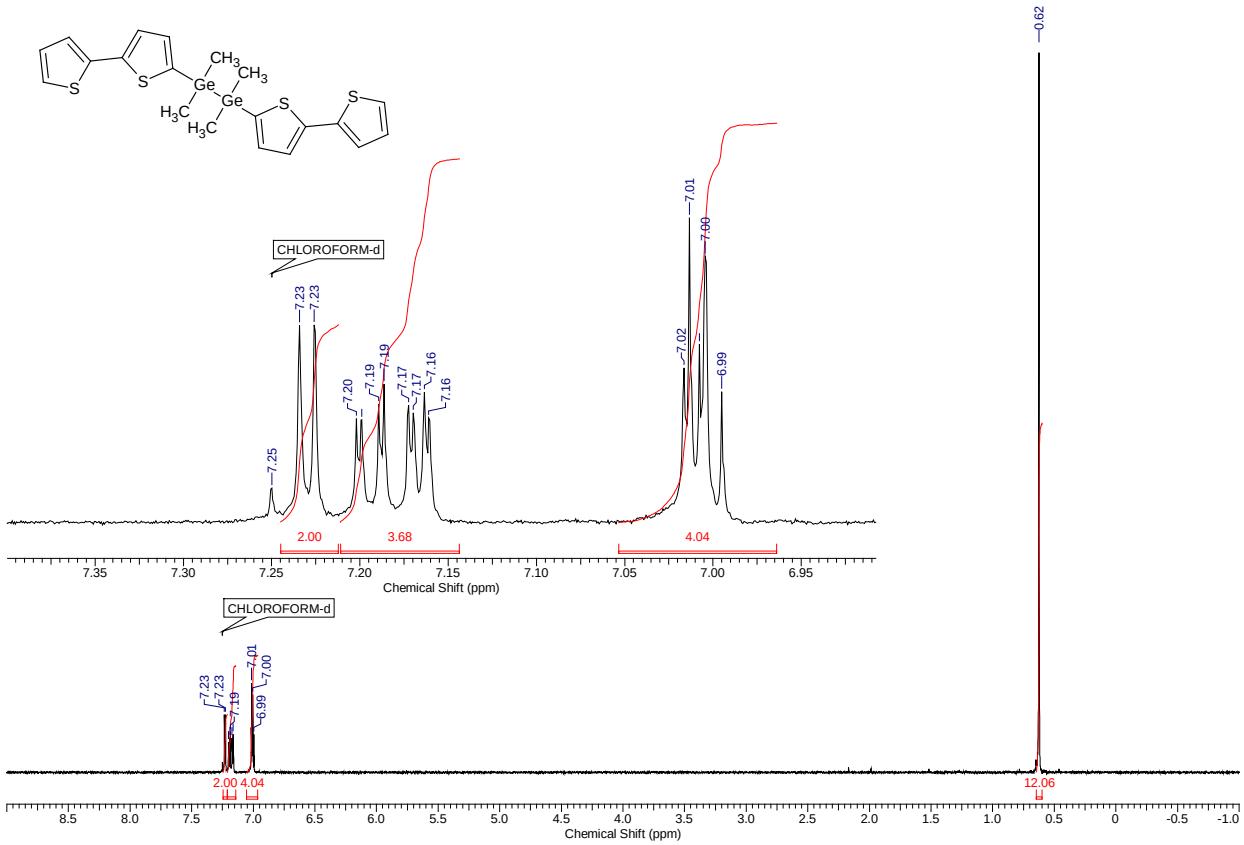


**Figure S32.** $^{1}$H NMR spectrum for **3b** ($CDCl_3$, RT).

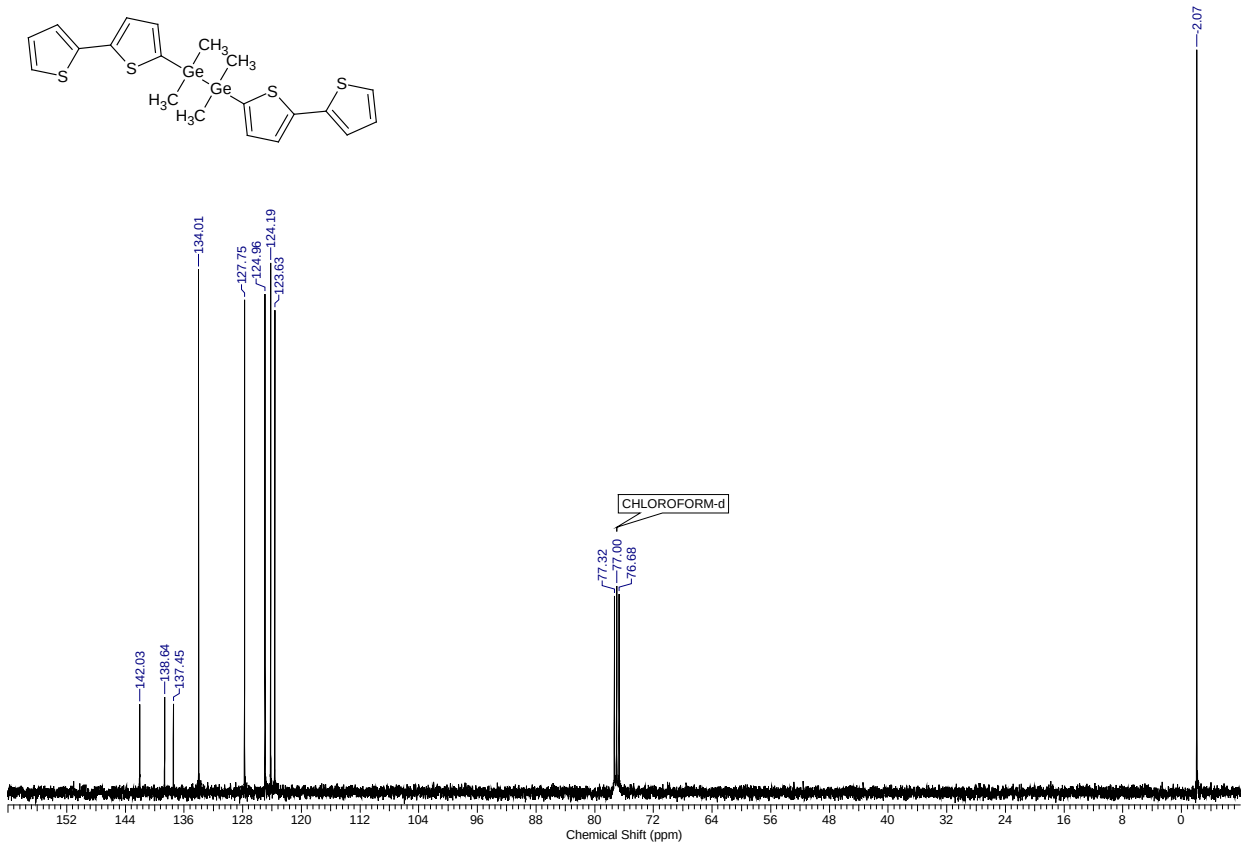


**Figure S33.** $^{13}$C NMR spectrum for **3b** ($CDCl_3$, RT).

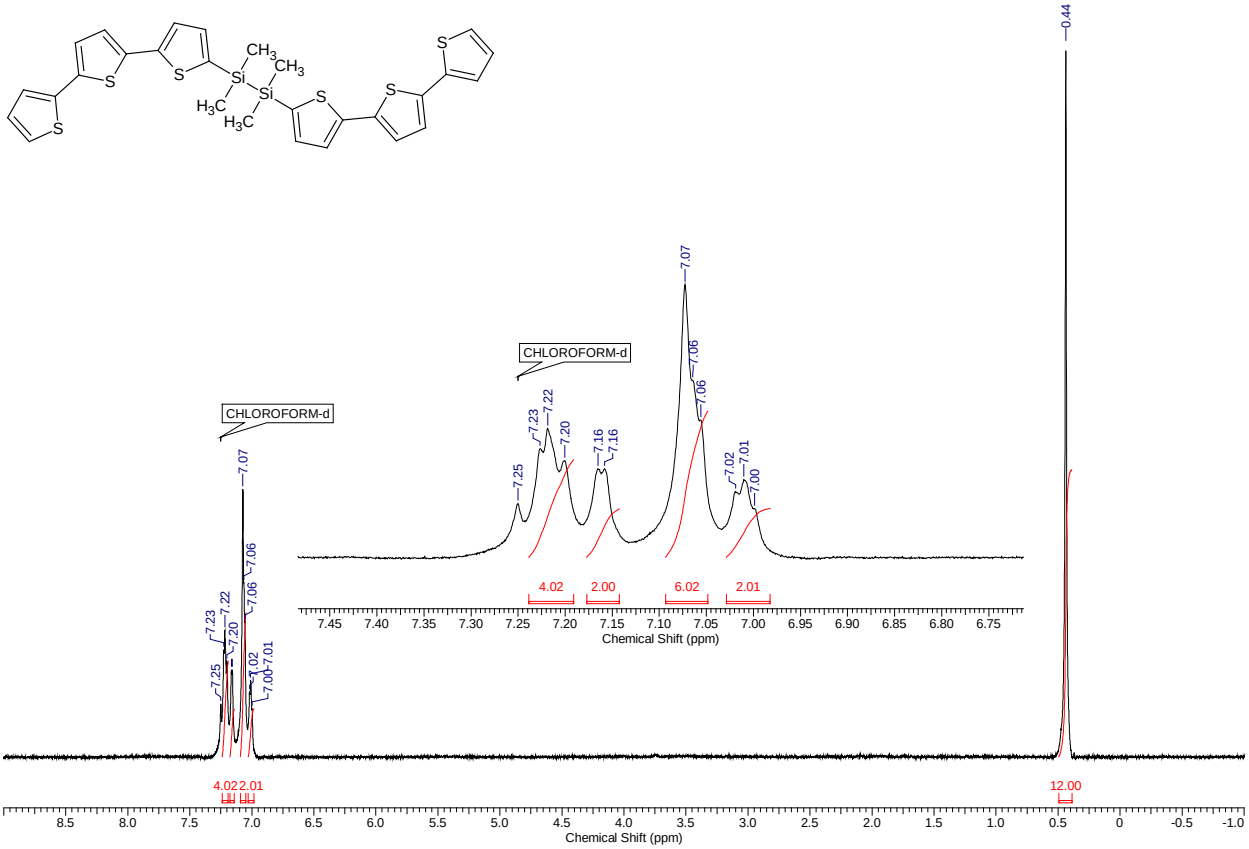


**Figure S34.** $^{1}$H NMR spectrum for **3c** ($CDCl_3$, RT).

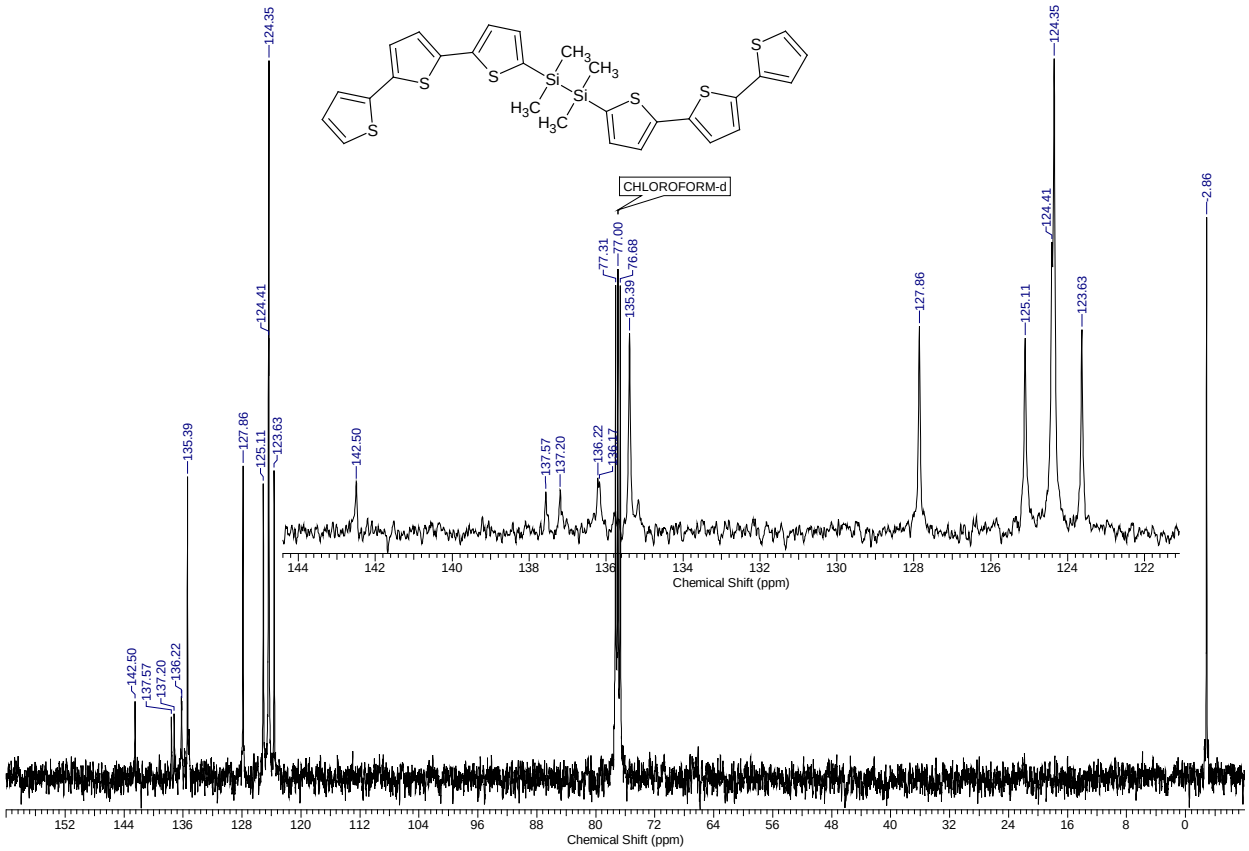


**Figure S35.** $^{13}$C NMR spectrum for **3c** ($CDCl_3$, RT).

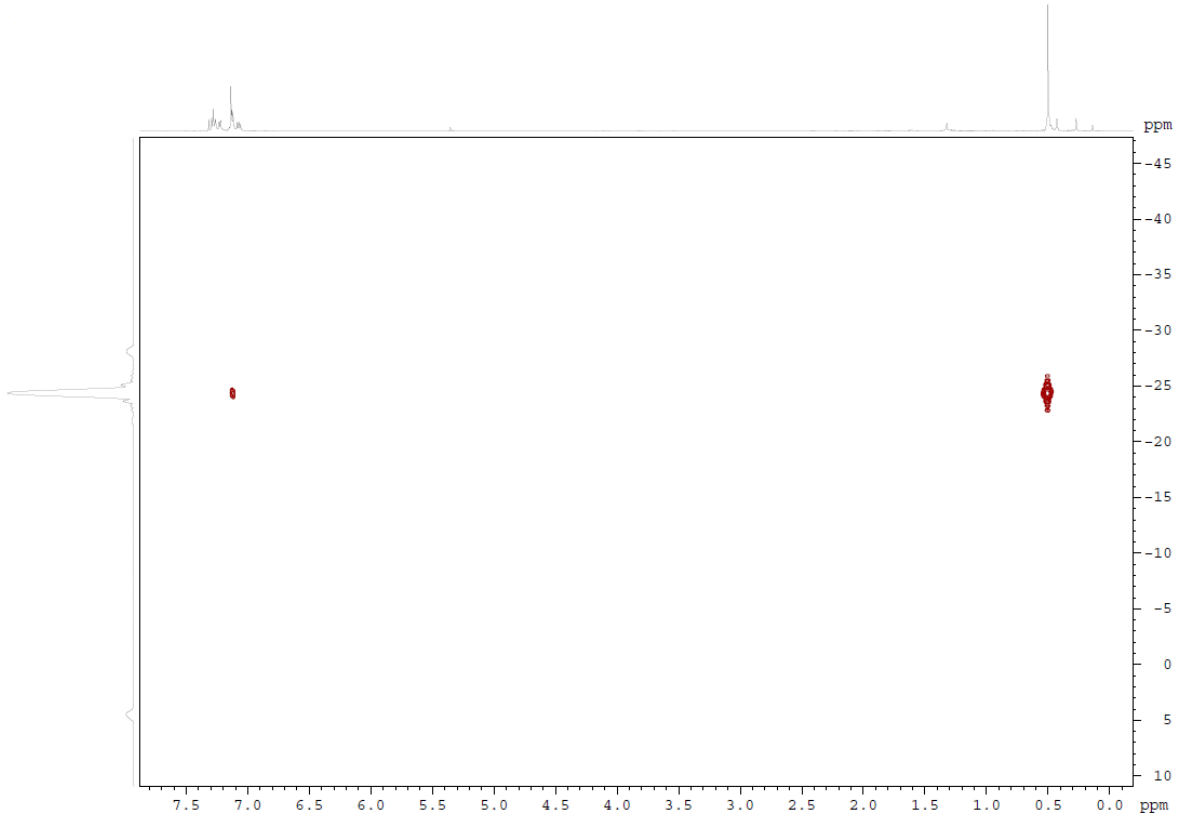


**Figure S36.** $^{29}$Si NMR spectrum for **3c** ($CDCl_3$, RT).

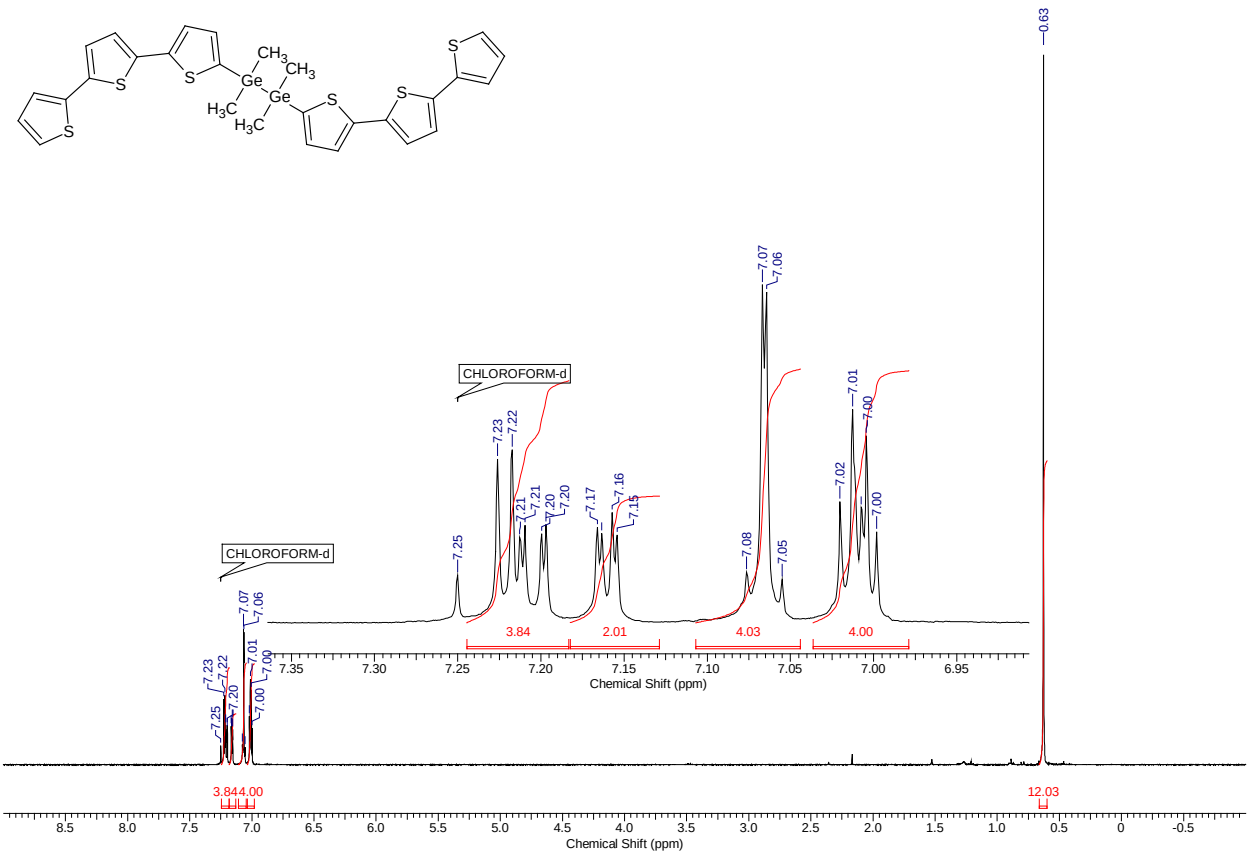


**Figure S37.** $^{1}$H NMR spectrum for **3d** ($CDCl_3$, RT).

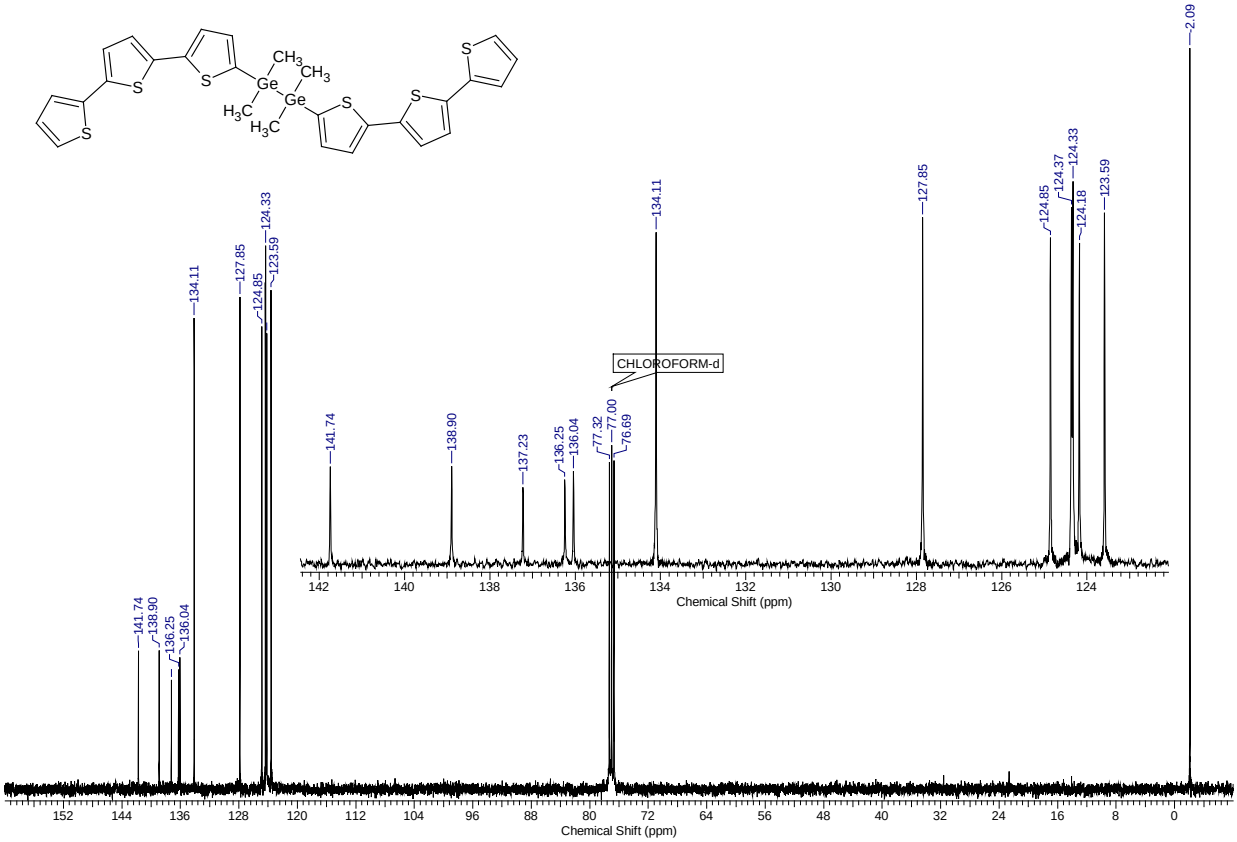


**Figure S38.** $^{13}$C NMR spectrum for **3d** ($CDCl_3$, RT).

## *UV/vis absorption and luminescence spectra*

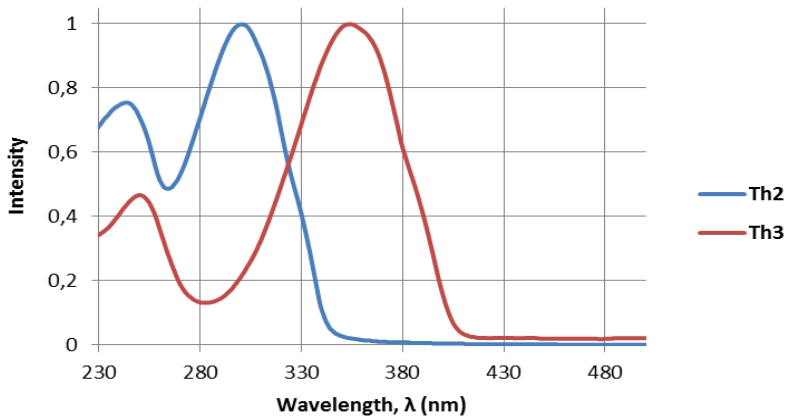


**Figure S39.** UV/vis absorption of $Th_2$ and $Th_3$ ($CH_2Cl_2$, room temperature).

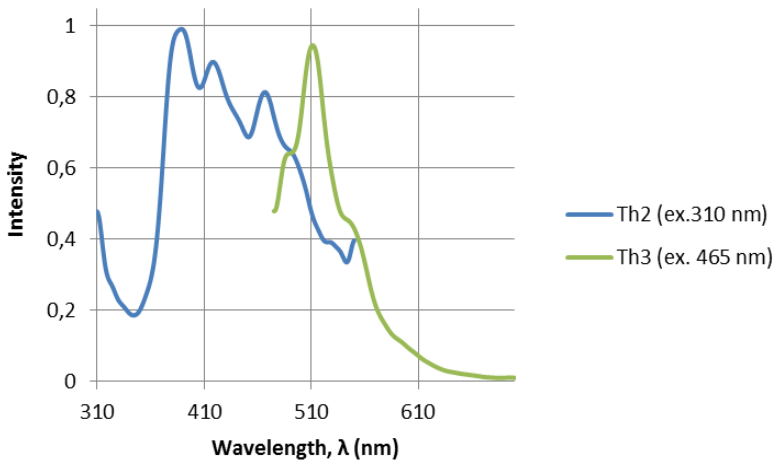


**Figure S40.** Emission of $Th_2$ and $Th_3$ in solid state (room temperature).

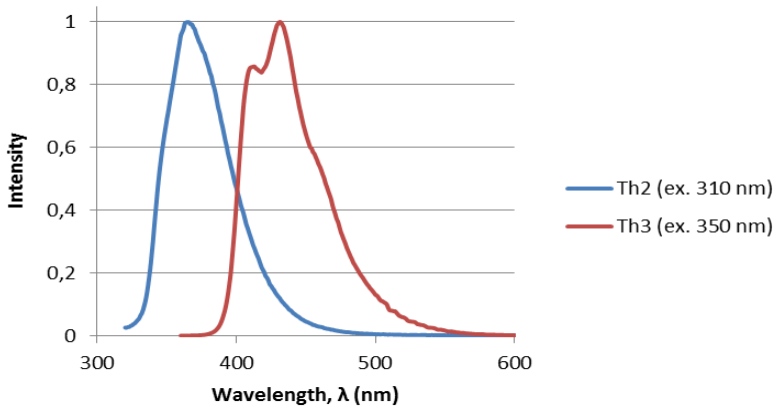


**Figure S41.** Emission of $Th_2$ and $Th_3$ in solution ($CH_2Cl_2$, room temperature).

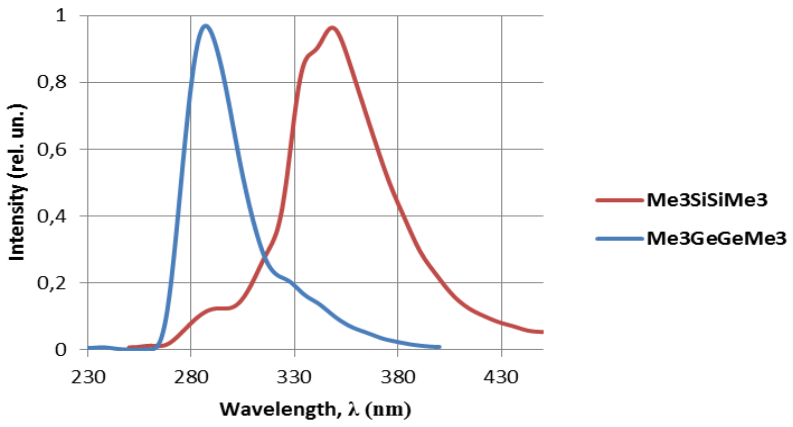


**Figure S42.** Emission of $Me_3SiSiMe_3$ and $Me_3GeGeMe_3$ in solution ($CH_2Cl_2$, room temperature).

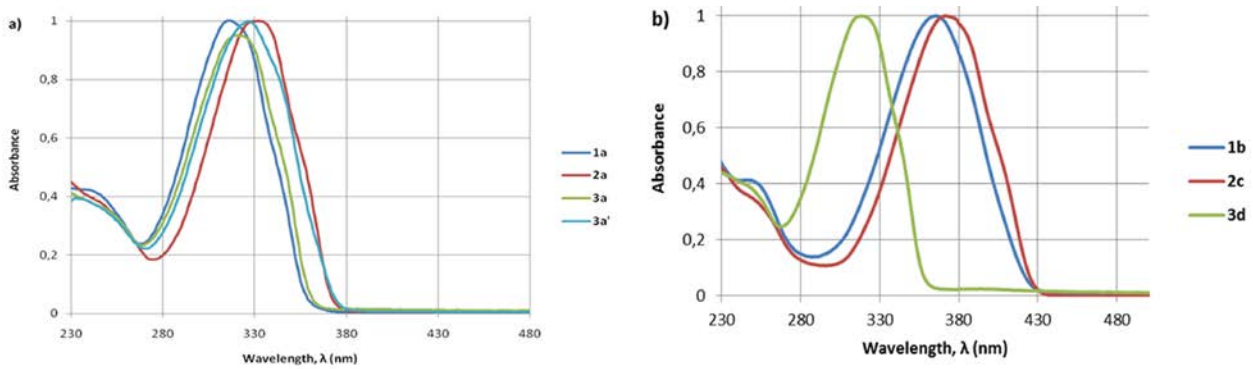


**Figure S43.** UV/visible absorption spectra ($CH_2Cl_2$, room temperature) for compounds: a) **1a**, **2a**, **3a**, and **3a'**; b) **1b**, **2c** and **3d**.

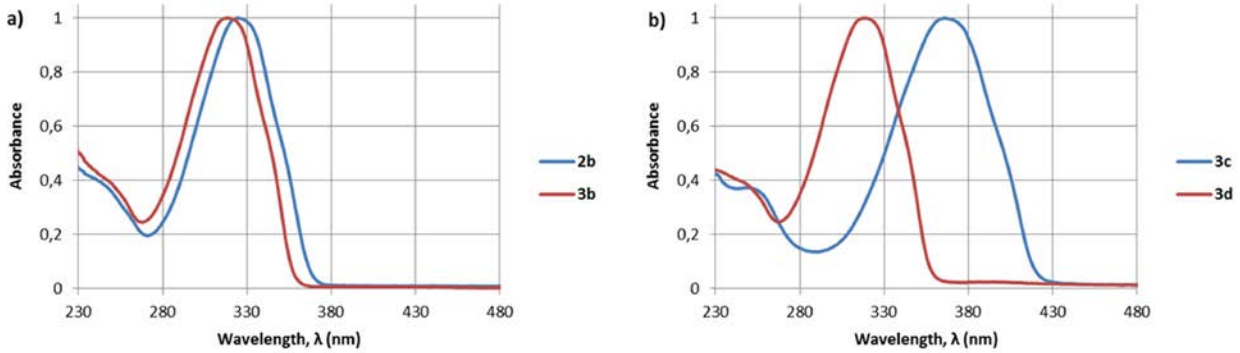


**Figure S44.** UV/visible absorption spectra ($CH_2Cl_2$, room temperature) for compounds: a) **2b** and **3b**; b) **3c** and **3d**.

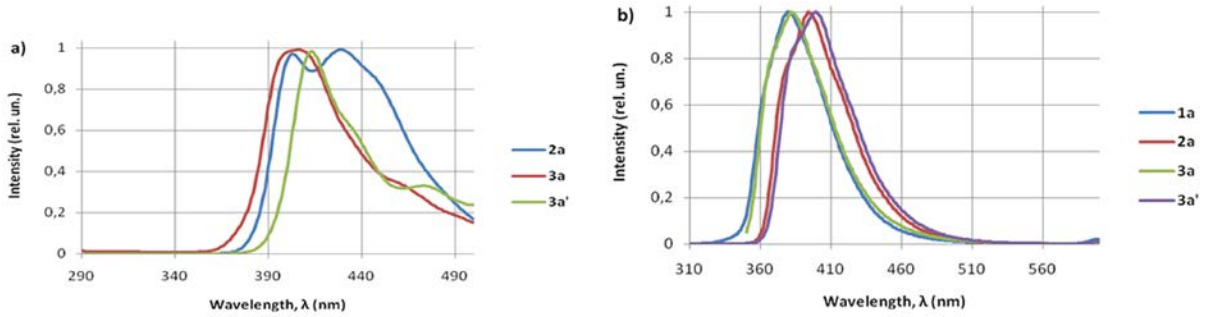


**Figure S45.** Luminescence emission for compounds **1a**, **2a**, **3a** and **3a'** at room temperature: a) in solid state; b) in solution ($CH_2Cl_2$).

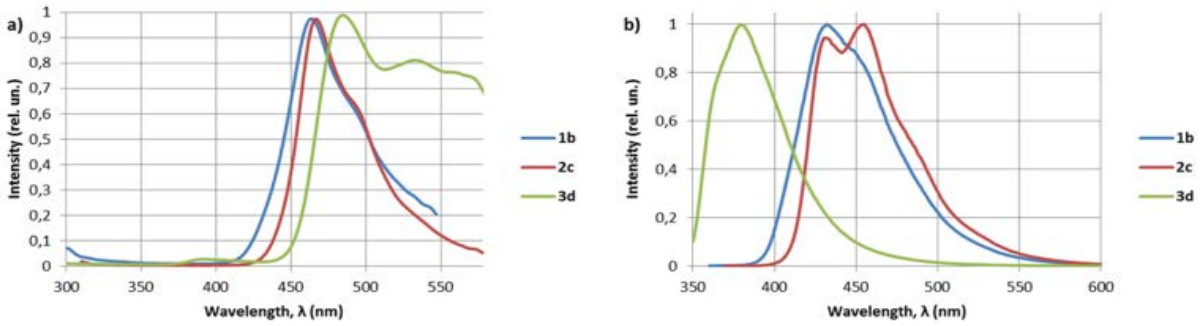


**Figure S46.** Luminescence emission for compounds **1b**, **2c**, and **3d** at room temperature: a) in solid state; b) in solution ($CH_2Cl_2$).

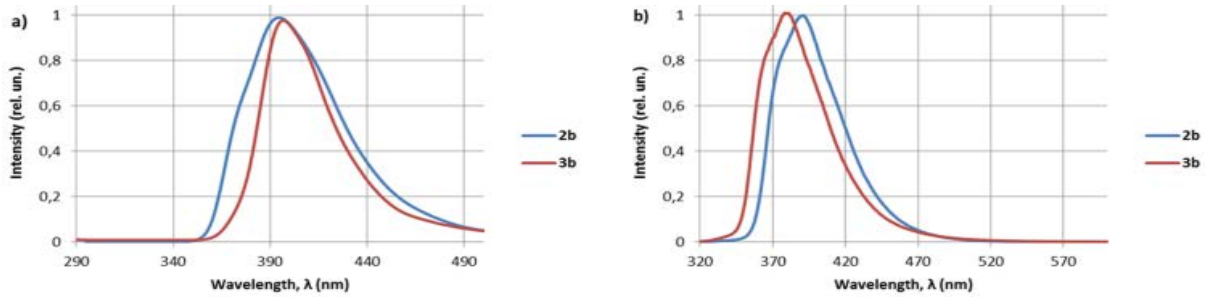


**Figure S47.** Luminescence emission for compounds **2b** and **3b** at room temperature: a) in solid state; b) in solution ($CH_2Cl_2$).

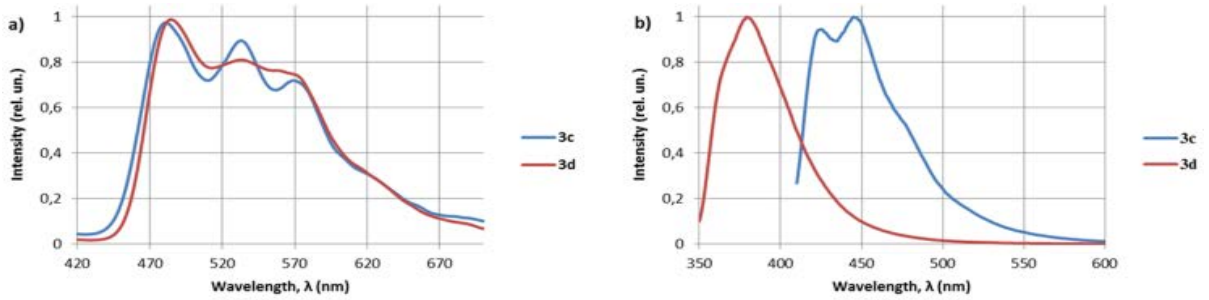


**Figure S48.** Luminescence emission for compounds **3c** and **3d** at room temperature: a) in solid state; b) in solution ($CH_2Cl_2$).

# ***DFT calculations***

**Description of the experiment**

The nonlocal hybrid three-parameter B3LYP[1] density functional has been used throughout the study because previous theoretical calculations have shown that B3LYP approach is a cost-effective method for studying metal containing systems.[2] Even at calculations of the thermodynamic parameters, B3LYP results compare well to the highly exact G2 (MP2, SVP) methods, as well as to the experimental values.[3] We have used PM3 level for large systems with phenyl and fluorophenyl rings. Than we have used the time-dependent density functional computations [6-31G(d) basis set], as implemented by Gaussian 09, were utilized to explore the excited manifold and compute the possible electronic transitions.

The calculations were performed with full geometry optimization and used the GAUSSIAN'09 program package.[4] The absence of imaginary vibration frequencies confirmed the stationary character of the structures.

**References**


1. Becke, A. D. *Phys. Rev. A* **1988**, *38*, 3098-3100.
2. Poleshchuk, O. K.; Shevchenko, E. L.; Branchadell, V.; Lein, M.; Frenking, G. *Int. J. Quantum Chem.* **2005**, *101*, 869-877.
3. Curtiss, L. A.; Raghavachari, K.; Redfern, P. C.; Pople, J. A. *J. Chem. Phys.* **1997**, *106*, 1063-1079.
4. Frisch, M. J. T., G. W.; Schlegel, H. B.; Gill, P. M. W.; Johnson, B. G.; Robb, M. A.; Cheeseman, J. R.; Keith, T.; Petersson, G. A.; Montgomery, J. A.; Raghavachari, K.; Al-Laham, M. A.; Zakrzewski, V.; Ortiz, J. V.; Foresman, J. B.; Closlowski, J.; Stefanov, B. B.; Nanayakkara, A.; Challacombe, M.; Peng, C. Y.; Ayala P. Y.; Chen, W.; Wong M. W.; Andress, J. L.; Replogle, E. S.; Gomperts, R.; Martin, R. L.; Fox, D. J.; Binkley, J. S.; Defress, D. J.; Baker, J.; Stewart, J. P.; Head-Gordon, Gonzales, C.; Pople, J. A. *Gaussian 09, Revision C.01; Gaussian, Inc: Pittsburg, PA,* **2010**.

**Table S2.** UV/vis absorption of a series of $Me_3\underline{M'}Me_2\underline{M}[Th]_n\underline{M}Me_2\underline{M'}Me_3$ (n= 1-3, M= Si, Ge, Sn).

| **M'** | **M** | **n** | **λ, nm** |
|---|---|---|---|
| Si | Si | 1 | 229 |
| | | 2 | 321 |
| | | 3 | 369 |
| | Ge | 1 | 252 |
| | | 2 | 322 |
| | | 3 | 369 |
| | Sn | 1 | 262 |
| | | 2 | 325 |
| | | 3 | 373 |
| Ge | Si | 1 | 247 |
| | | 2 | 317 |
| | | 3 | 366 |
| | Ge | 1 | 247 |
| | | 2 | 318 |
| | | 3 | 367 |
| | Sn | 1 | 256 |
| | | 2 | 318 |
| | | 3 | 370 |

**Table S3.** UV/vis absorption data for$Th_2MMe_2M'Me_2Th_2$ [B3LYP/6-31+G(d,p)].

| M | M' | **λ, nm UV** | relation |
|---|---|---|---|
| Si | Si | 325 | HOMO-LUMO |
| | Ge | 327 | HOMO-LUMO |
| | | 321 (i) | HOMO-LUMO+1 |
| | Sn | 331 | HOMO-LUMO |
| | | 321 (i) | HOMO-LUMO+1 |
| Ge | Ge | 314 | HOMO-LUMO |
| | | 312 | HOMO-LUMO+1 |
| | | 298 (i) | HOMO-1-LUMO+1 |
| | Sn | 325 | HOMO-LUMO |
| | | 321 (i) | HOMO-LUMO+1 |
| Sn | Sn | 321 | HOMO-LUMO |
| | | 318 (i) | HOMO-LUMO+1 |

**Table S4.** UV/vis absorption and luminescence data according DFT calculations.

| Compound | Absorbance | | | | Fluorescence | | |
|---|---|---|---|---|---|---|---|
| | $\lambda_{abs}$, nm | oscillator strength | transition | HOMO/LUMO energy, eV [a] | $\lambda_{em}$, nm | oscillator strength | transition |
| $Si_2Th_2Si_2$ (**2a**) | 355 | 0.88 | HOMO - LUMO | -5.67/-1.71 (313) | 459 | 1.00 | LUMO - HOMO |
| | 281 | 0.01 | HOMO-1 – LUMO | | 315 | 0.03 | LUMO – HOMO-1 |
| | 270 | 0.02 | HOMO – LUMO+1 | | 316 | 0.32 | LUMO+1 - HOMO |
| | | | | | 292 | 0.03 | LUMO – HOMO-2 |
| $Ge_2Th_2Ge_2$ (**2b**) | 350 | 0.88 | HOMO - LUMO | -5.62/-1.60 (308) | 455 | 1.00 | LUMO - HOMO |
| | 279 | 0.01 | HOMO-1 – LUMO | | 313 | 0.03 | LUMO – HOMO-1 |
| | 272 | 0.02 | HOMO – LUMO+1 | | 316 | 0.30 | LUMO+1 -HOMO |
| | | | | | 292 | 0.03 | LUMO – HOMO-2 |
| $Th_2Si_2Th_2$ (**3a**) | 353 | 1.00 | HOMO - LUMO | -5.73/-1.76 (312) | 452 | 1.00 | LUMO - HOMO |
| | 331 | 0.09 | HOMO – LUMO+1 | | 405 | 0.11 | LUMO+1 - HOMO |
| | 320 | 0.04 | HOMO-1 – LUMO | | 378 | 0.09 | LUMO – HOMO-1 |
| | 309 | 0.25 | HOMO-1 – LUMO+1 | | 354 | 0.26 | LUMO+1 – HOMO-1 |
| $Th_2Ge_2Th_2$ (**3b**) | 346 | 1.00 | HOMO - LUMO | -5.72/-1.69 (308) | 443 | 1.00 | LUMO - HOMO |
| | 329 | 0.11 | HOMO – LUMO+1 | | 394 | 0.20 | LUMO+1 - HOMO |
| | 317 | 0.04 | HOMO-1 – LUMO | | 376 | 0.06 | LUMO – HOMO-1 |
| | 308 | 0.24 | HOMO-1 – LUMO+1 | | 350 | 0.31 | LUMO+1 – HOMO-1 |

[a] gap in nm in parentheses

**Table S5.** Calculated UV/vis absorption and luminescence data for $Me_3GeGeMe_2[Th]_nGeMe_2GeMe_3$.

| | Absorption | | | Luminescence | |
|---|---|---|---|---|---|
| n | λ, nm | Transition | HOMO/LUMO (eV) | λ, nm | Transition |
| 1 | 262 | homo→lumo | -6.46/-1.22 | 394 | LUMO-HOMO |
| 2 | 344 | homo→lumo | -5.89/-1.82 | 452 | LUMO-HOMO |
| 3 | 407 | homo→lumo | -5.59/-2.12 | 561 | LUMO-HOMO |
| 4 | 456 | homo→lumo | -5.42/-2.29 | 651 | LUMO-HOMO |
| 5 | 494 | homo→lumo | -5.31/-2.39 | 728 | LUMO-HOMO |
| 6 | 531 | homo→lumo | -5.23/-2.49 | 791 | LUMO-HOMO |
| 7 | 551 | homo→lumo | -5.19/-2.53 | 832 | LUMO-HOMO |
| 8 | 570 | homo→lumo | -5.15/-2.57 | 841 | LUMO-HOMO |
| 9 | 589 | homo→lumo | -5.12/-2.60 | | |

**Table S6.** Calculated UV/vis absorption data for $Th(Th)_nGeMe_2GeMe_2(Th)_nTh$.

| n | λ, nm | Transition | HOMO/LUMO (eV) |
|---|---|---|---|
| 0 | 270 | HOMO→LUMO | -6.12/-0.98 |
| 1 | 346 | HOMO→LUMO | -5.73/-1.69 |
| 2 | 419 | HOMO→LUMO | -5.46/-2.09 |
| 3 | 476 | HOMO→LUMO | -5.31/-2.31 |
| 4 | 523 | HOMO→LUMO | -5.21/-2.46 |
| 6 | 595 | HOMO→LUMO | -5.09/-2.63 |

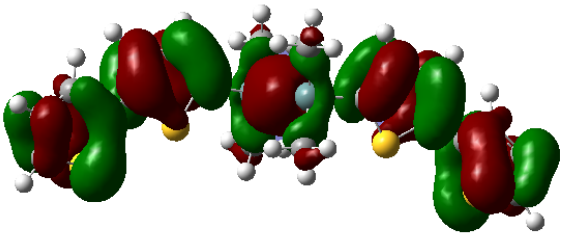

**Figure S49.** HOMO molecular orbital for $Th_2Ge_2Me_4Th_2$.

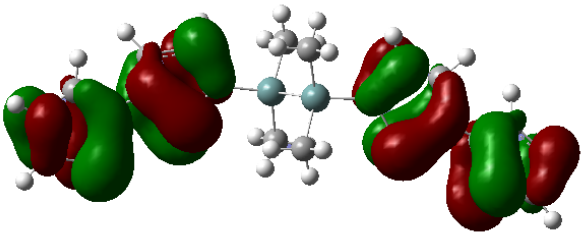

**Figure S50.** HOMO-1 molecular orbital for $Th_2Ge_2Me_4Th_2$.

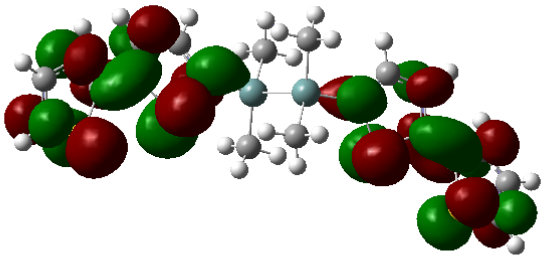

**Figure S51.** LUMO molecular orbital for $Th_2Ge_2Me_4Th_2$.

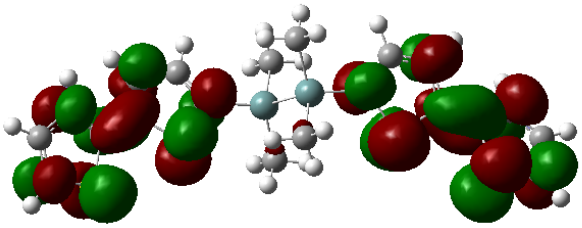

**Figure S52.** LUMO+1 molecular orbital for $Th_2Ge_2Me_4Th_2$.

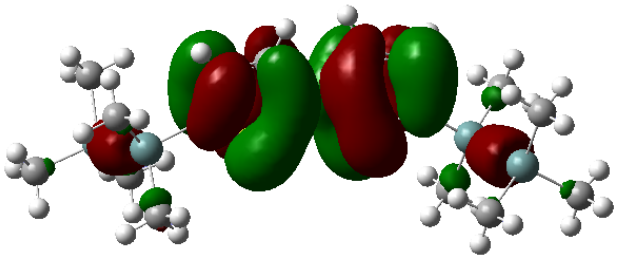

**Figure S53.** HOMO molecular orbital for $Me_5Ge_2Th_2Ge_2Me_5$.

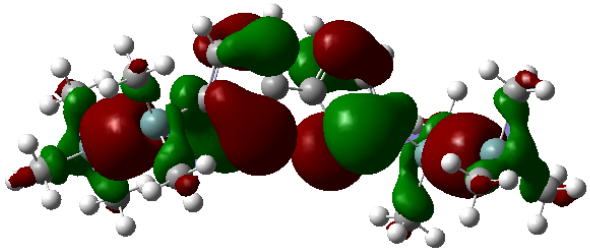

**Figure S54.** HOMO-1 molecular orbital for $Me_5Ge_2Th_2Ge_2Me_5$.

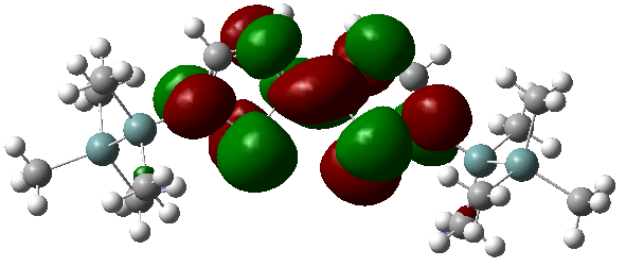

**Figure S55.** LUMO molecular orbital for $Me_5Ge_2Th_2Ge_2Me_5$.

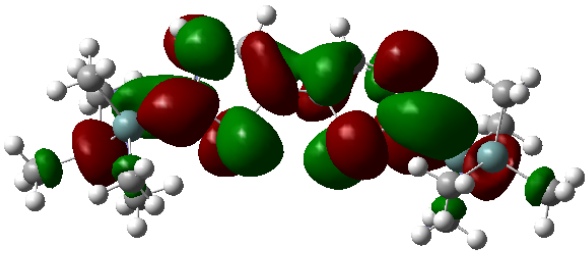

**Figure S56.** LUMO+1 molecular orbital for $Me_5Ge_2Th_2Ge_2Me_5$.

# ***Electrochemical data according to CV***

**Description of the experiment**

Electrochemical measurements were carried out using an Autolab 302N potentiostat interfaced through Nova 2.0 software to a personal computer. Electrochemical measurements were performed in a glovebox under oxygen levels of less than 5 ppm using solvent that had been purified by passing through an alumina-based purification system. Diamond-polished glassy carbon electrodes of 3 mm diameter were employed for cyclic voltammetry (CV) scans. CV data were evaluated using standard diagnostic criteria for diffusion control and for chemical and electrochemical reversibility. The experimental reference electrode was a silver wire coated with anodically deposited silver chloride and separated from the working solution by a fine glass frit. The electrochemical potentials in this paper are referenced to ferrocene/ferrocenium couple, as recommended elsewhere.[1] The ferrocene potential was obtained by its addition to the analyte solution.[2] At an appropriate time in the experiment $[NBu_4][B(C_6F_5)_4]$ was prepared as previously described.[3]

## References


1. G. Gritzner and J. Kuta, *Pure Appl. Chem.*, 1984, **56**, 461.

2. R.R. Gagne, C.A. Koval, G.C. Lisensky, *Inorg. Chem.* 1980, **19**, 2854.

3. K. Lam, K.; W.E. Geiger, *J. Organomet. Chem.* 2016, **817**, 15.


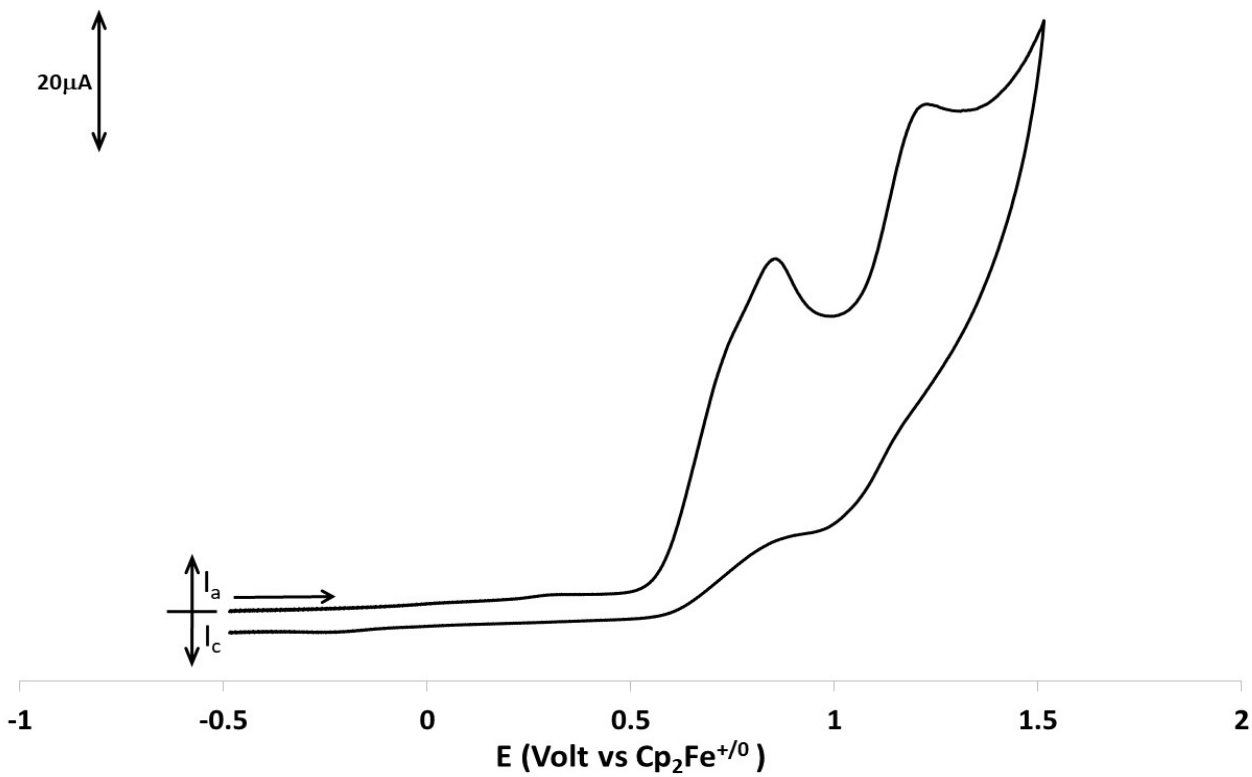


**Figure S57.** Cyclic voltammogram of 1.0 mM **2a** in dichloromethane - $[NBu_4]$[TFAB] solution. Sweeping rate 200 mV/s at room temperature (ox. wave). 3 oxidation peaks ($E_{pa}$= 0.73, 0.85 and 1.21 V *vs.* $Fc^+$/Fc).

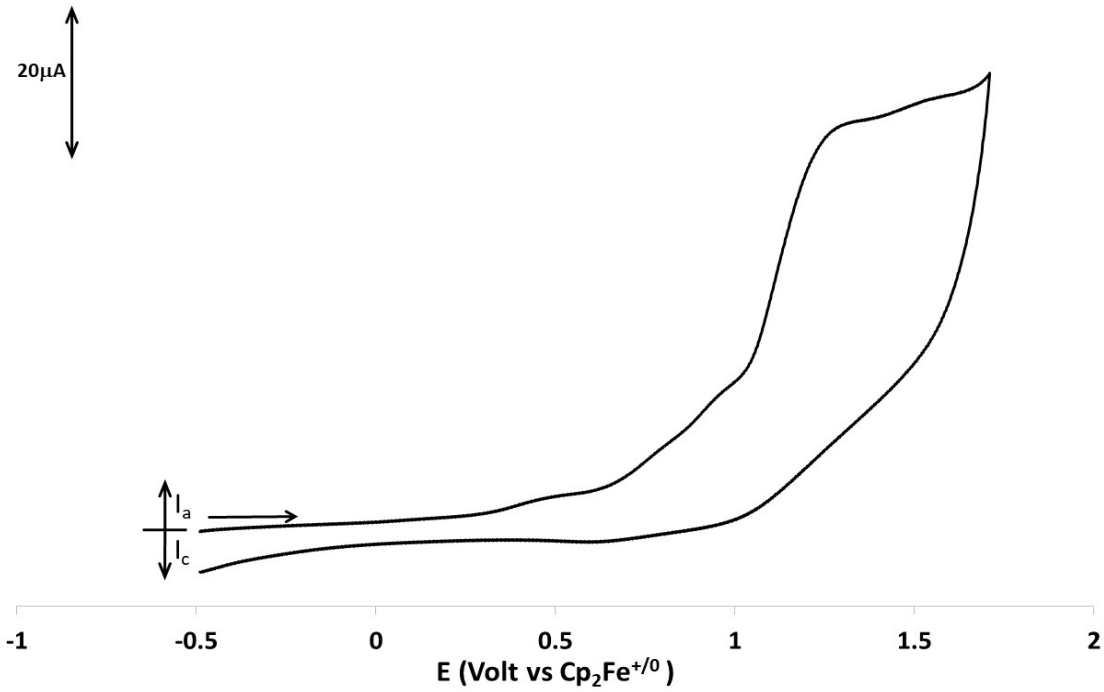


**Figure S58.** Cyclic voltammogram of 1.0 mM **2b** in dichloromethane - [$NBu_4$][TFAB] solution. Sweeping rate 200 mV/s at room temperature (ox. wave). 3 oxidation peaks ($E_{pa}$= 0.80, 0.95, 1.29 V *vs.* $Fc^+$/Fc).

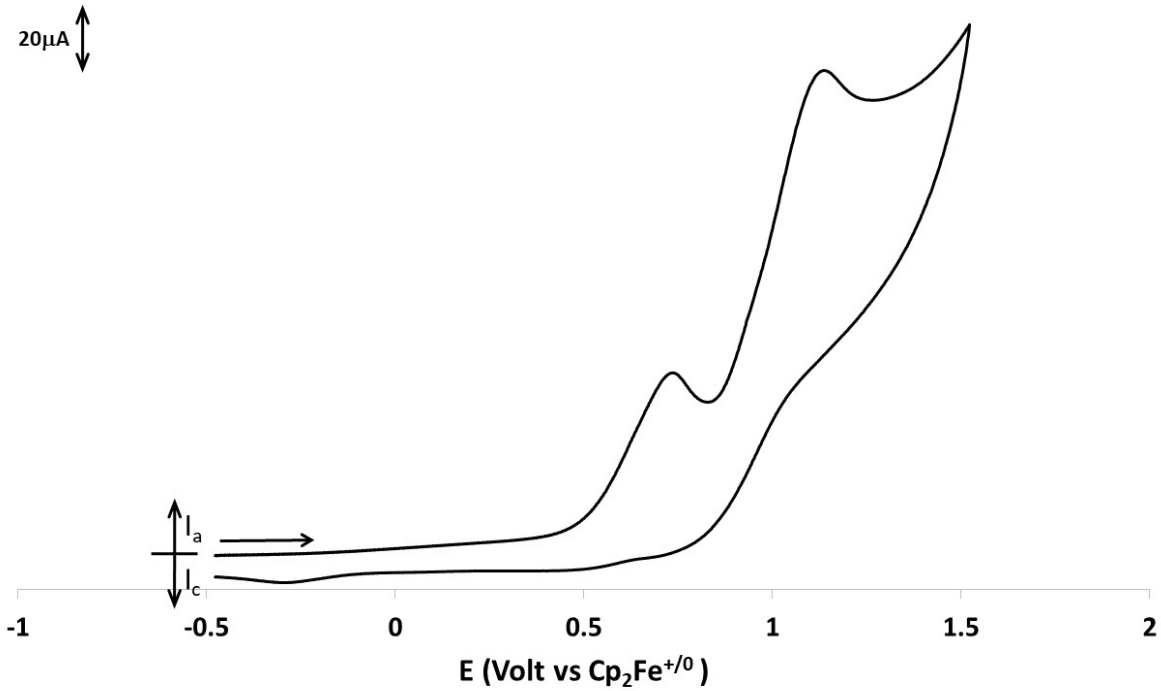


**Figure S59.** Cyclic voltammogram of 1.0 mM **3a** in dichloromethane - [$NBu_4$][TFAB] solution. Sweeping rate 200 mV/s at room temperature (ox. wave). 2 oxidation peaks ($E_{pa}$= 0.73 and 1.14 V *vs.* $Fc^+$/Fc).

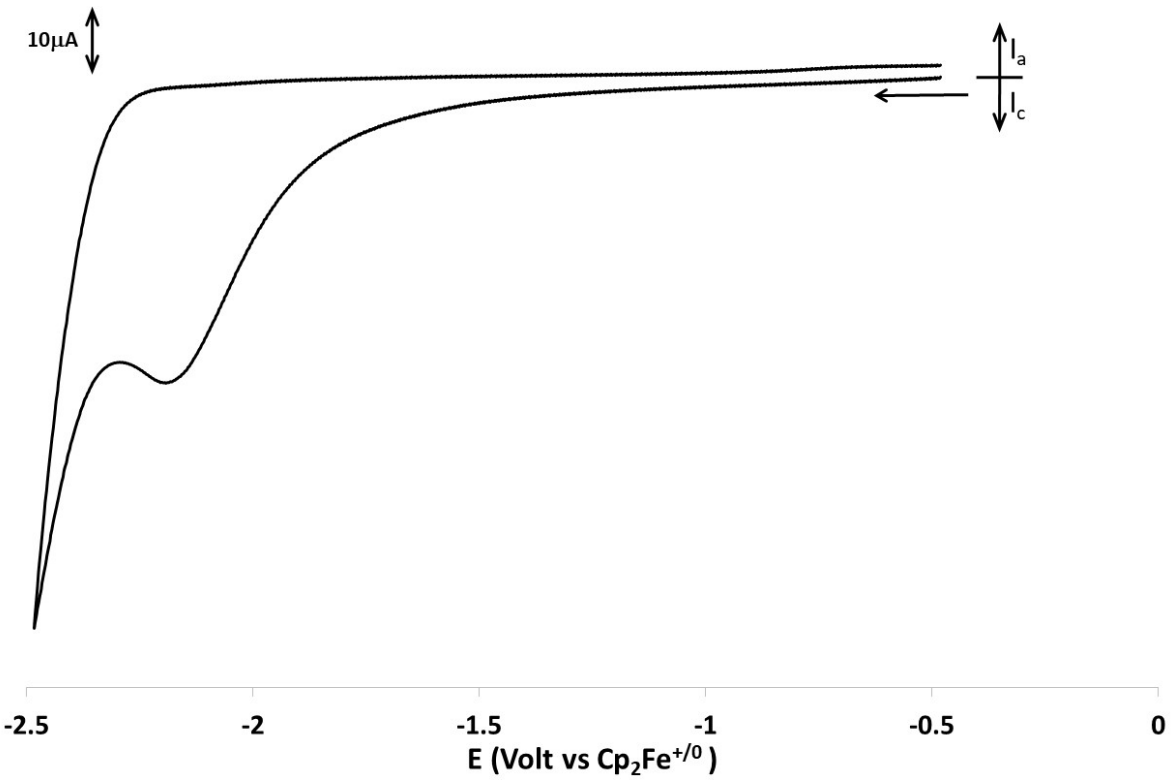


**Figure S60.** Cyclic voltammogram of 1.0 mM **3a** in dichloromethane - [$NBu_4$][TFAB] solution. Sweeping rate 200 mV/s at room temperature (red. wave). 1 reduction peak ($E_{pc}$= -2.20 V *vs.* $Fc^+$/Fc).

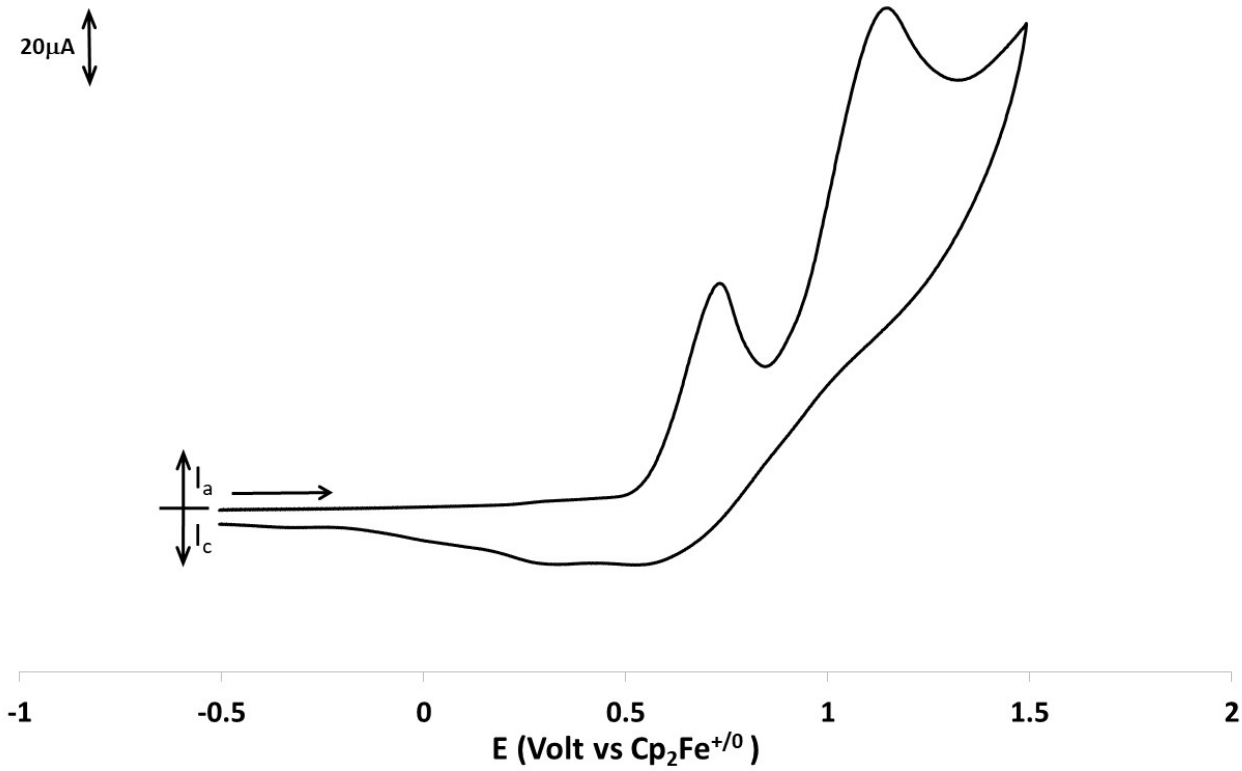


**Figure S61.** Cyclic voltammogram of 1.0 mM **3b** in dichloromethane - [$NBu_4$][TFAB] solution. Sweeping rate 200 mV/s at room temperature (ox. wave). 2 oxidation peaks ($E_{pa}$= 0.73 and 1.15 V *vs.* $Fc^+$/Fc).

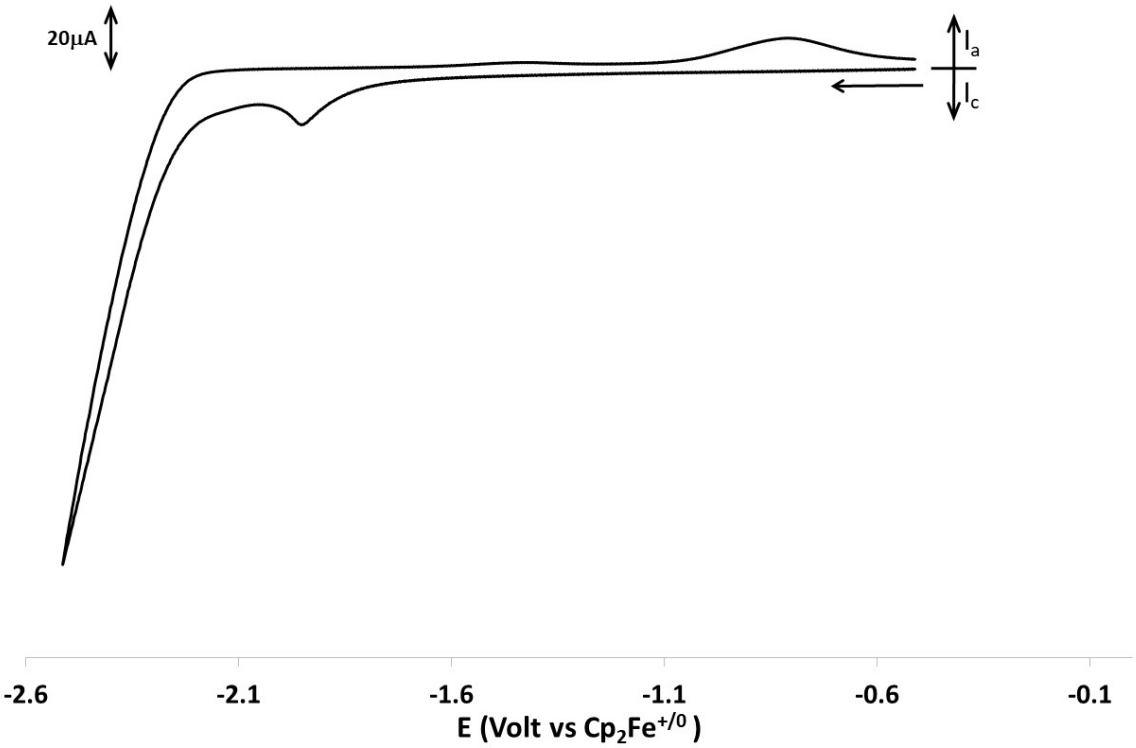


**Figure S62.** Cyclic voltammogram of 1.0 mM **3b** in dichloromethane - [$NBu_4$][TFAB] solution. Sweeping rate 200 mV/s at room temperature (red. wave). 1 reduction peak ($E_{pc}$= -1.95 V *vs.* $Fc^+$/Fc) and 1 reoxidation peak ($E_{pa}$= -0.80 V *vs.* $Fc^+$/Fc).

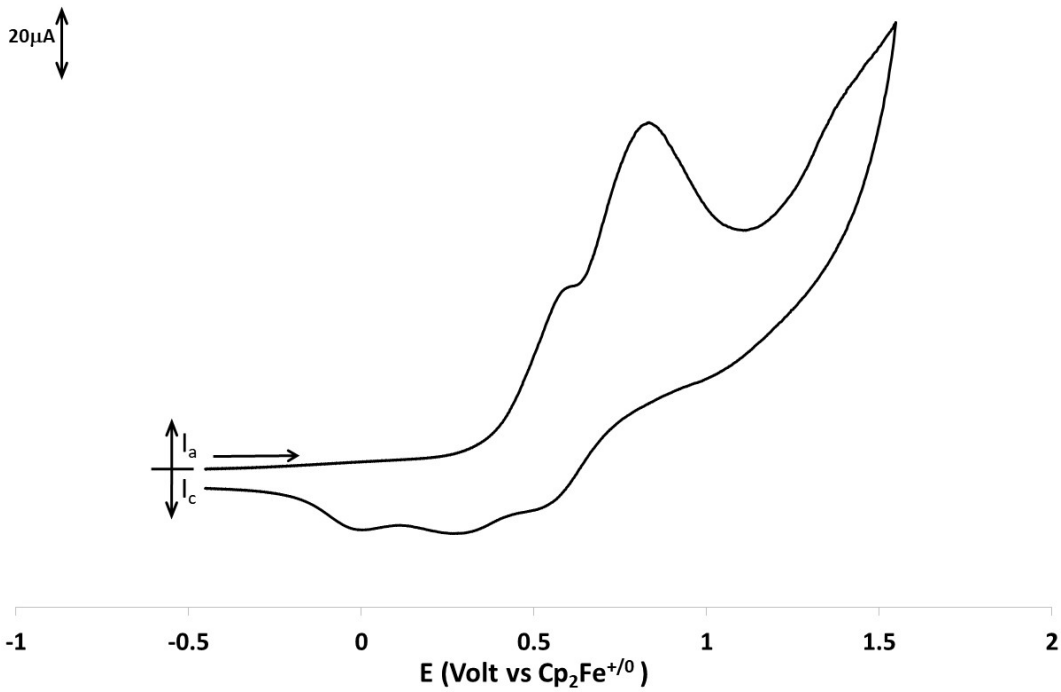


**Figure S63.** Cyclic voltammogram of 1.0 mM **3c** in dichloromethane - [$NBu_4$][TFAB] solution. Sweeping rate 200 mV/s at room temperature (ox. wave). 3 oxidation peaks ($E_{pa}$= 0.58, 0.83 and 1.38 V *vs.* $Fc^+$/Fc) and 3 rereduction peaks ($E_{pc}$= -0.01, 0.30 and 0.54 V *vs.* $Fc^+$/Fc).

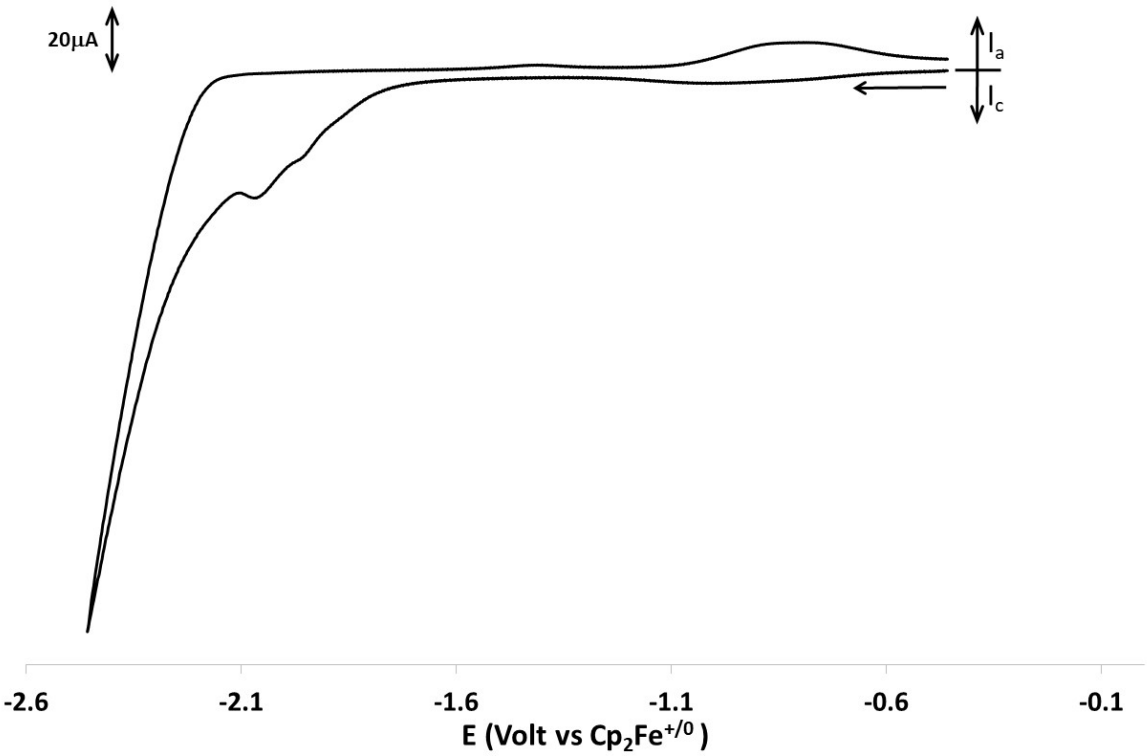


**Figure S64.** Cyclic voltammogram of 1.0 mM **3c** in dichloromethane - [$NBu_4$][TFAB] solution. Sweeping rate 200 mV/s at room temperature (red. wave). 2 reduction peaks ($E_{pc}$= -1.96, -2.10 V *vs.* $Fc^+$/Fc) and 1 reoxidation peak ($E_{pa}$= -0.81 V *vs.* $Fc^+$/Fc).

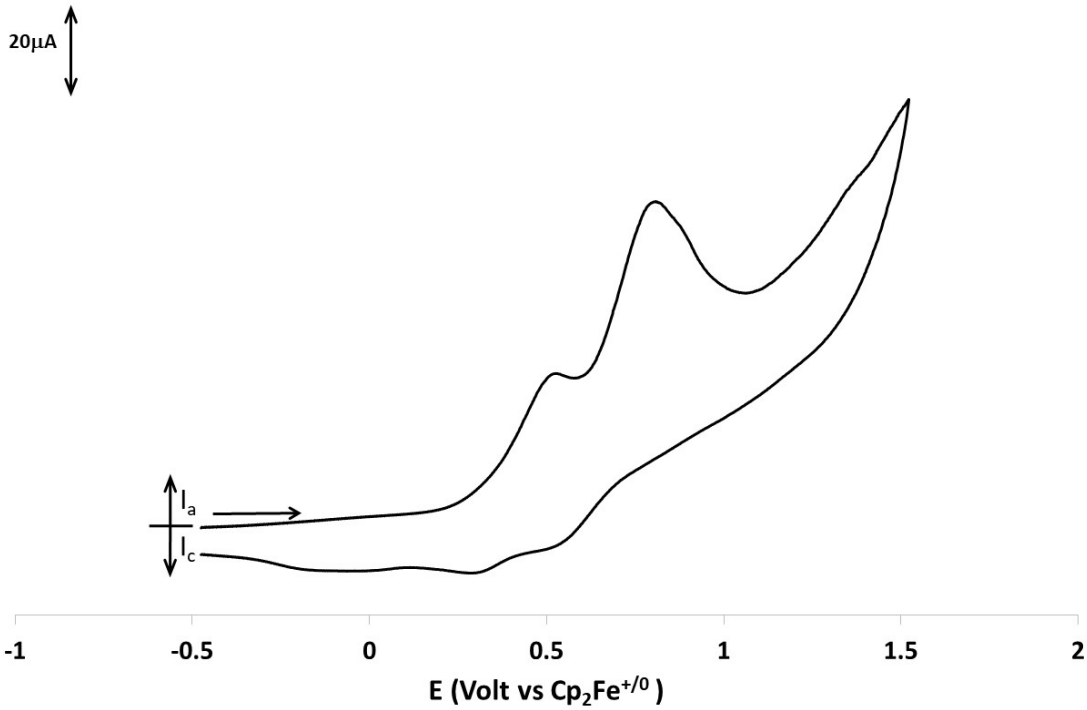


**Figure S65.** Cyclic voltammogram of 1.0 mM **3d** in dichloromethane - [$NBu_4$][TFAB] solution. Sweeping rate 200 mV/s at room temperature (ox. wave). 3 oxidation peaks ($E_{pa}$= 0.51, 0.79 and 1.38 V *vs.* $Fc^+$/Fc) and 2 rereduction peaks ($E_{pc}$= 0.53 and 0.30 V *vs.* $Fc^+$/Fc).

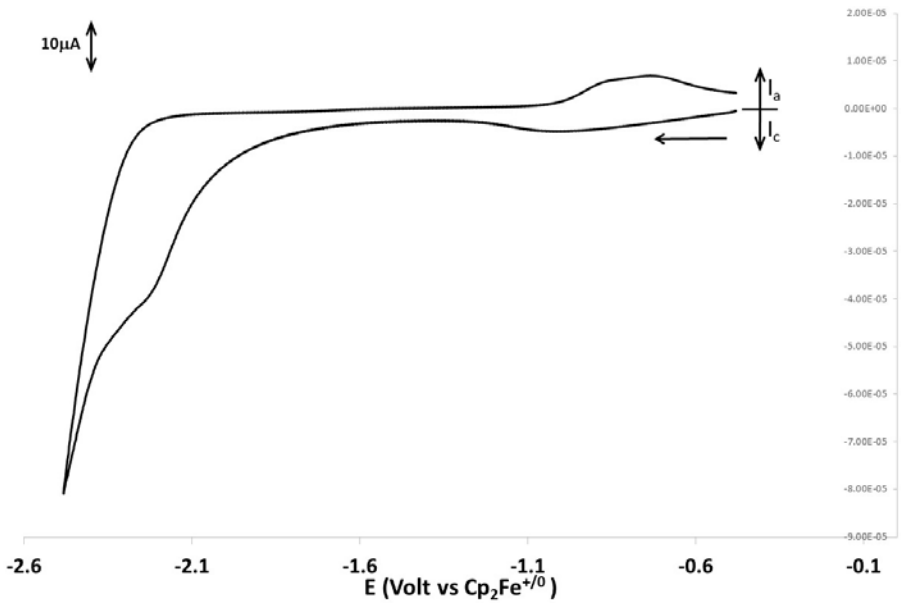


**Figure S66.** Cyclic voltammogram of 1.0 mM **3d** in dichloromethane - [$NBu_4$][TFAB] solution. Sweeping rate 200 mV/s at room temperature (red. wave). 2 reduction peaks ($E_{pc}$= -1.01 and -2.22 V *vs.* $Fc^+$/Fc) and 2 reoxidation peaks ($E_{pa}$= -0.86 and -0.72 V *vs.* $Fc^+$/Fc).

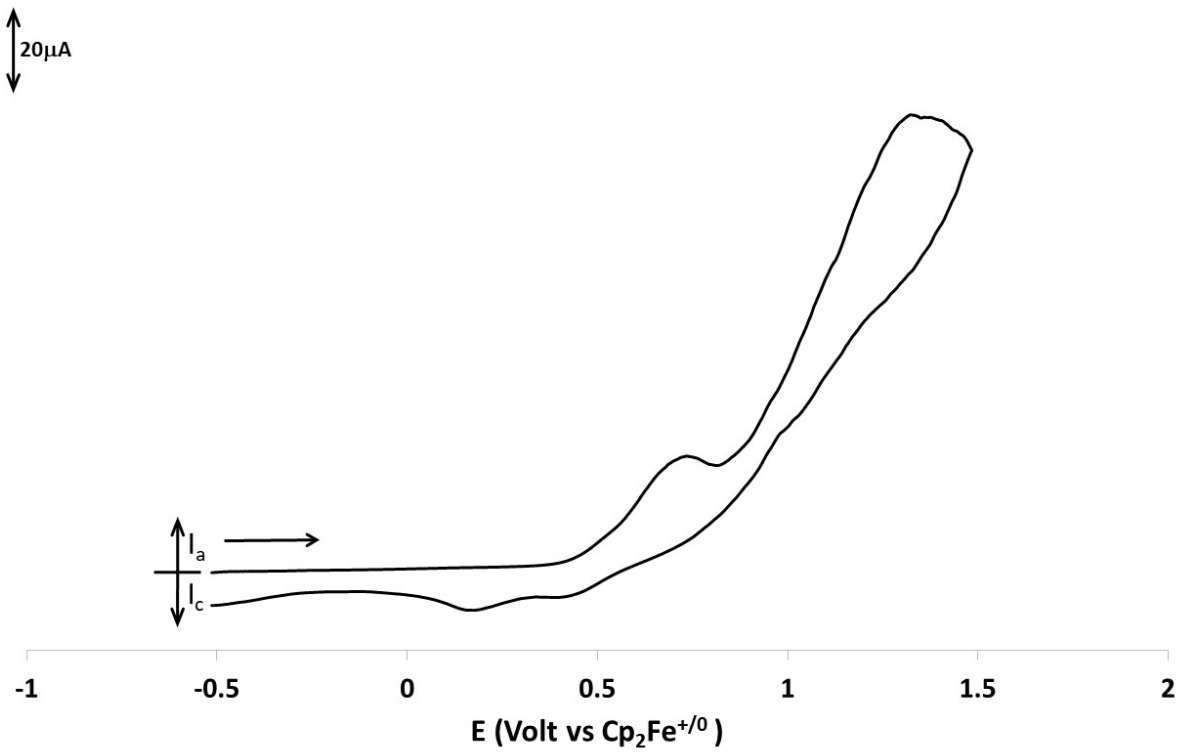


**Figure S67.** Cyclic voltammogram of 1.0 mM **3a'** in dichloromethane - [$NBu_4$][TFAB] solution. Sweeping rate 200 mV/s at room temperature. 2 oxidation peaks ($E_{pa}$= 0.73 and 1.33V *vs.* $Fc^+$/Fc) and 2 rereduction peaks ($E_{pc}$= 0.17 and 0.42 V *vs.* $Fc^+$/Fc).

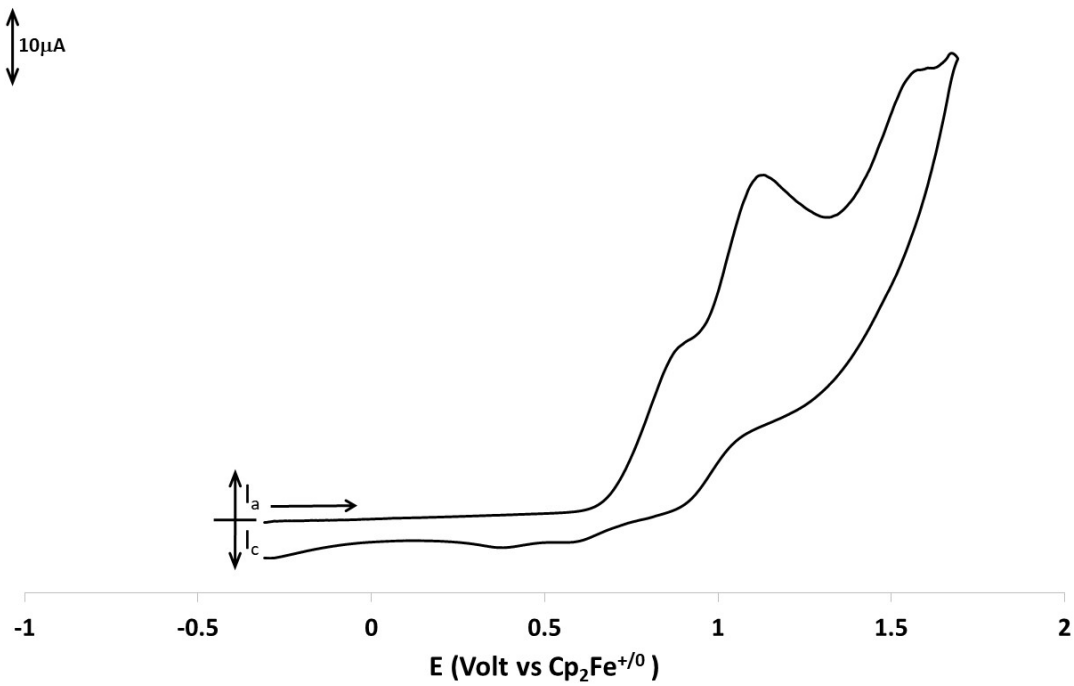


**Figure S68.** Cyclic voltammogram of 0.7 mM **5** in dichloromethane - [$NBu_4$][TFAB] solution. Sweeping rate 200mV/s at room temperature (ox. wave). 3 oxidation peaks ($E_{pa}$= 0.90, 1.12 and 1.58 V *vs.* $Fc^+$/Fc) and 2 rereduction peaks ($E_{pc}$= 0.37 and 0.60 V *vs.* $Fc^+$/Fc).